RSC Advances

REVIEW

View Article Online
View Journal | View Issue

Cite this: *RSC Adv.*, 2025, **15**, 22180

Research progress on the preparation, performance, mechanisms, and applications of carbon nanomaterials against Gram-negative bacteria

Chengwei Zhang, †[b] Ying Zheng,†[a] Xiaoyan Lin[a] and Shaohuang Weng *[a]

The excessive and inappropriate use of antibiotics in clinical settings has led to bacterial mutations and the emergence of drug resistance. This escalating problem presents a major challenge in the treatment of infections, particularly those caused by Gram-negative and multidrug-resistant bacteria, for which effective therapeutic options are increasingly limited. As a result, there is an urgent need to develop novel antimicrobial agents. Recent studies have demonstrated that carbon nanomaterials, owing to their potent antibacterial activity and low susceptibility to resistance, are emerging as promising candidates in antimicrobial research. This review provides a comprehensive overview of recent advancements in the synthesis strategies, antibacterial efficacy against Gram-negative bacteria, underlying antimicrobial mechanisms, and biomedical applications of four main carbon nanomaterials (CNMs) of graphene quantum dots (GQDs), carbon dots (CDs), carbon nanotubes (CNTs), and graphene. The preparation methods and antibacterial mechanisms of CNMs with antibacterial properties are the main section. Additionally, the review addresses the current challenges hindering their clinical translation and explores potential future directions with a focus on efficacy and safety. By collating current findings, this review aims to establish a theoretical foundation for the development of innovative antimicrobial agents targeting Gram-negative bacteria.

Received 10th March 2025
Accepted 20th June 2025

DOI: 10.1039/d5ra01704a

rsc.li/rsc-advances

1. Introduction

Since the discovery of penicillin by Alexander Fleming in 1929, the development of a vast array of antimicrobial agents has significantly advanced global public health.[1] However, the widespread, excessive, and inappropriate use of antibiotics has led to the emergence of antibiotic-resistant bacterial strains.[2] In response to this growing threat, the World Health Organization (WHO) published a list of priority antibiotic-resistant pathogens in 2017, classifying them into critical, high, and medium priority groups.[3] Alarmingly, some of these pathogens have developed resistance to nearly all available antibiotics, posing a severe threat to human health and survival.[4]

Owing to their unique structural characteristics, Gram-negative bacteria exhibit a higher propensity for developing antibiotic resistance compared to Gram-positive bacteria, contributing to increased morbidity and mortality rates worldwide.[5] Notably, the majority of the WHO-designated priority resistant pathogens belong to the Gram-negative group. These bacteria possess a distinctive three-layered cell envelope, a key factor in their resistance mechanisms. The outermost layer, the outer membrane (OM), is a defining feature of Gram-negative bacteria and serves as a protective barrier against external threats.[6] The inner leaflet of the OM consists of phospholipids, while the outer leaflet contains lipopolysaccharides (LPS), which are known to trigger endotoxin shock in humans.[7] Additionally, the OM is embedded with outer membrane proteins (OMPs), which allow small molecules like amino acids and sugars to pass through. Beneath the OM lies the peptidoglycan cell wall, a rigid exoskeleton composed of repeating units of *N*-acetylglucosamine and *N*-acetylmuramic acid, which maintains cell shape and structural integrity.[8] The innermost layer is the inner membrane (IM), a phospholipid bilayer that not only offers structural support but also plays a crucial role in molecular transport, biosynthesis, and cellular division by anchoring DNA and facilitating sister-chromatid separation.[9] The OM plays a pivotal role in bacterial resistance to a wide range of antibiotics, including β-lactams, quinolones, and polymyxins. Structural modifications in the OM, such as alterations in porin hydrophobicity or mutations in membrane components, can significantly reduce antibiotic permeability and enhance resistance.[10] In contrast, Gram-positive bacteria lack this protective OM, rendering them generally more

[a]*Department of Pharmaceutical Analysis, School of Pharmacy, Fujian Medical University, Fuzhou 350122, P. R. China. E-mail: shweng@fjmu.edu.cn*
[b]*School of Basic Medical Sciences, Fujian Medical University, Fuzhou, 350122, China*
† Equally contributed.

susceptible to antibiotics.[11–13] Consequently, treatment options for infections caused by multidrug-resistant Gram-negative bacteria are becoming increasingly limited.

Gram-negative bacteria are responsible for severe infections in humans, particularly in individuals with weakened or underdeveloped immune systems, such as neonates, the elderly, and patients undergoing surgery or cancer treatments. These infections are often associated with high morbidity and mortality rates.[14] Antibiotic-resistant infections caused by Gram-negative bacteria have emerged as one of the most formidable challenges in clinical medicine.[15] Notably, drug-resistant Gram-negative bacteria are the primary pathogens responsible for ventilator-associated pneumonia, catheter-associated bloodstream infections, and other intensive care unit (ICU)-acquired sepsis, including urinary tract infections.[16] Alarmingly, recent WHO reports on novel antibiotic formulations indicate that of the 50 new antimicrobial agents currently under development, only a small fraction exhibit efficacy against Gram-negative bacteria. In response to the growing threat of antibiotic resistance, various strategies have been explored to combat Gram-negative and multidrug-resistant bacteria *via* diverse molecular mechanisms. These approaches include the development of novel antibiotics,[17] derivatives of existing antibiotics,[18,19] antibiotic adjuvants,[20] antimicrobial peptides derived from mammals and other organisms[21] and lipopeptides and its assembly.[22–24] Among these approaches, antimicrobial peptides designed from venom peptides have demonstrated considerable promise due to their potent therapeutic properties.[25,26]

Nevertheless, despite initial efficacy, bacterial populations eventually develop resistance, reinforcing concerns about the so-called "post-antibiotic era"—a looming global health crisis that underscores the urgent need for innovative antimicrobial agents to combat drug-resistant Gram-negative bacteria.[27] In recent decades, rapid advances in nanotechnology have provided promising alternatives for antimicrobial therapy.[28] Among these, carbon nanomaterials (CNMs) have attracted significant attention due to their diverse synthesis methods, unique structural features, favourable physicochemical properties, and relatively high biocompatibility. These materials are primarily composed of carbon atoms, which can form single bonds through sp^3 hybridization as well as stable double and triple bonds through sp^2 and sp hybridization, enabling the formation of various allotropes with distinct structures and properties.[29] Notable examples of CNMs include zero-dimensional graphene quantum dots, carbon quantum dots (CQDs), one-dimensional carbon nanotubes, and two-dimensional graphene. As research on CNMs has progressed, their intrinsic physicochemical properties, such as large surface area and nanoscale dimensions, have been found to confer unique antibacterial capabilities. These attributes enable CNMs to inhibit or eliminate microbial populations while minimizing the risk of bacterial resistance. Consequently, their application has broadened the scope of nanomaterial-based antimicrobial research, offering novel strategies for the development of effective antibacterial agents. Furthermore, CNMs are relatively easy to synthesize, require inexpensive and abundantly available raw materials, and hold significant potential for antimicrobial therapy.

Despite the growing body of research on the antibacterial properties of CNMs, considerable challenges remain in their clinical application, particularly in their use against Gram-negative bacteria. Given the continuous advancements in antimicrobial nanomaterials, it is essential to systematically review and evaluate the potential of carbon-based nanomaterials for addressing Gram-negative bacterial infections. This review focuses on the research progress of four key CNMs—graphene quantum dots (GQDs), carbon dots (CDs), carbon nanotubes (CNTs), and graphene—with respect to their antibacterial activity against Gram-negative bacteria. The discussion encompasses their synthesis methods, physicochemical properties, antibacterial mechanisms, and current biomedical applications. Finally, the challenges associated with the practical application of these CNMs in antimicrobial therapy are examined, along with potential future research directions.

2. Preparation of antibacterial carbon nanomaterials

The antibacterial properties of CNMs are intricately linked to their microstructure and surface chemical characteristics, which are primarily influenced by their preparation methods. These methods can generally be categorized into two main approaches: top-down and bottom-up.

2.1 Top-down preparation methods

The top-down method involves the breakdown of larger carbon materials into nanoscale particles or structures through physical or chemical processes. The fundamental principle of this approach is to begin with bulk materials and progressively reduce their size *via* physical actions or chemical reactions, ultimately yielding nanostructures.[30]

2.1.1 Laser ablation. The laser ablation technique utilizes high-energy laser pulses directed at the surface of macromolecular carbon-based materials. This process rapidly heats, melts, and evaporates the material into a plasma state, followed by vapor crystallization to form CDs.[31] This method offers several advantages, including excellent adaptability, environmental friendliness, and high purity.[32] However, it also exhibits certain drawbacks, such as high energy consumption, the uncontrolled production of CDs with varying sizes, and low quantum yields (QYs).[33] In 2006, Sun *et al.*[34] first synthesized GQDs *via* the laser ablation of graphite. Subsequently, Santiago *et al.*[35] successfully prepared nitrogen-doped GQDs using polylactic acid and polyethylene glycol (PEG) as organic precursors. These nitrogen-doped GQDs exhibited an average particle size of approximately 3.4 nm and a nitrogen-to-carbon atomic ratio as high as 26%. The incorporation of nitrogen significantly enhanced the photoluminescence efficiency of the GQDs, opening new avenues for their applications. With ongoing research on CQDs, the influence of laser parameters—such as laser intensity, pulse width, and ablation duration—on the properties of CQDs has become a focal point of investigation. As

a result, there is a growing emphasis on developing efficient and uniform CQDs preparation methods. For example, Nguyen *et al.*[36] achieved precise control over the size distribution and photoluminescence characteristics of CQDs by finely adjusting laser density, spot size, and irradiation time. To further improve the efficiency and uniformity of CQDs preparation, Cui *et al.*[37] introduced a dual-beam pulsed laser ablation technique. By splitting the laser beam using a beam splitter, this method significantly reduced ablation time and markedly improved the efficiency of CQDs production. Compared to the traditional single-beam pulsed laser ablation, the CQDs produced by the dual-beam method exhibited more uniform sizes, enhanced monodispersity, and a QY of up to 35.4%, demonstrating the clear advantages of this technique. In subsequent studies, Nguyen *et al.*[38] utilized dual-pulse femtosecond laser ablation to synthesize CDs with an average size of only 1 nm, further enhancing their potential applications in sensing and catalysis. Additionally, Menazea *et al.*[39] employed pulsed laser ablation technology to embed silver nanoparticles (AgNPs) and CuO NPs into graphene oxide (GO), thereby preparing AgNPs@GO and CuONPs@GO composites. These materials exhibited significant photocatalytic antibacterial activity against *Escherichia coli* (*E. coli*) and *Staphylococcus aureus* (*S. aureus*), leading to bacterial death through disruption of the bacterial cell membrane. Furthermore, Khashan *et al.*[40] used pulsed laser ablation in liquid to fabricate CNTs modified with iron oxide nanoparticles. These composites demonstrated strong antibacterial activity against various bacterial strains, inducing bacterial membrane damage and cell death *via* the physical disruption of CNTs and the chemical action of the iron oxide nanoparticles.

2.1.2 Electric arc discharge. The arc discharge method has emerged as a prominent technique for the preparation of CDs since its first application by Xu *et al.*[41] in 2004, and it has since garnered widespread attention. The principle of this method involves using pure graphite electrodes to generate an arc discharge in distilled water, which results in the production of CDs. During this process, bubbles formed around the arc act as miniature reactors, thereby facilitating the reaction in an aqueous environment isolated from atmospheric interference. This unique preparation method yields products that can be categorized into three distinct phases: floating materials, suspensions, and precipitates. The suspensions predominantly consist of CDs, along with a small amount of GO sheets. Following synthesis, the floating materials are removed, and the water is left undisturbed for 24 hours to allow larger particles to settle. Subsequently, the suspended CDs are separated from the precipitates.[42] Despite the innovative nature of the arc discharge method, several challenges persist. Firstly, the process is labour-intensive, costly, and demands meticulous attention, particularly during the purification stages.[43] The high temperatures and energies generated during the arc discharge can introduce impurities, which may negatively affect the performance of the CDs. Furthermore, while CDs synthesized *via* this method exhibit excellent fluorescence properties, they often suffer from uneven particle sizes and low overall yields, which significantly limit their potential for large-scale production.[44,45] In addition, Li *et al.*[46] synthesized low-toxicity and biodegradable CDs using ascorbic acid (VC) *via* electrochemical methods. These CDs demonstrated broad-spectrum antibacterial and antifungal activity against various bacteria and fungi, leading to microbial death by damaging cell walls and binding to DNA/RNA to suppress gene expression. Meanwhile, Liu *et al.*[47] developed silver–iron/single-walled carbon nanotubes (Ag–Fe/SWCNTs) through direct current hydrogen arc discharge. These composites exhibited excellent antibacterial activity against *E. coli*, with Ag^+ ion release and physical disruption of the bacterial cell membrane contributing to their antibacterial effects. The high crystallinity of the SWCNTs and the high loading of Ag/Fe nanoparticles further enhanced the antibacterial efficacy of the composites.

2.1.3 Ultrasonic synthesis. The ultrasonic synthesis method generates microbubbles in solution through alternating high-pressure and low-pressure waves. The cavitation of these microbubbles induces strong fluid dynamic shear forces, which fragment large carbon-based nanomaterials—such as graphite, activated carbon, and CNTs—into nanoscale CDs.[48] This method is widely recognized for its low cost, simplicity, and non-toxic nature.[49] In 2012, Zhuo *et al.*[50] first synthesized GQDs *via* ultrasonic exfoliation of graphene, demonstrating the feasibility of this technique for nanomaterial fabrication. The ultrasonic method has also been employed in the synthesis of heteroatom-doped GQDs. For instance, Huang *et al.*[51] successfully prepared chlorine-doped GQDs through ultrasonic exfoliation of chlorinated carbon fiber (CF) precursors, providing new insights into the functionalization of GQDs. Traditionally, amine-functionalized CDs (NH_2-CDs) have been synthesized using hydrothermal methods, which are often complex and costly due to challenges in controlling chemical reactions. In contrast, Wu *et al.*[52] developed a simplified ultrasonic synthesis approach to produce NH_2-CDs, significantly reducing production costs while expanding potential applications in cellular imaging and metal ion sensing. They employed anhydrous ammonium citrate as the precursor, *N*,*N*-dimethylformamide (DMF) as a modifier, and water as the solvent. Under the synergistic influence of ultrasound, high temperature, and pressure, the precursor solution underwent rapid condensation and carbonization reactions, leading to the successful synthesis of high-performance CDs. These CDs exhibited high fluorescence quantum yields, stable luminescence properties, and tuneable spectral characteristics, highlighting their broad application potential in lighting displays, bioimaging, photocatalysis, environmental monitoring, and information storage and transmission. Additionally, the research team pioneered the integration of biomimetic design with advanced numerical simulation techniques to optimize microchannel structures, significantly enhancing fluid flow uniformity and energy transfer efficiency. Furthermore, they innovatively developed an ultrasonic microreactor system, wherein a piezoelectric transducer was directly coupled with the microreactor to ensure efficient and uniform transmission of ultrasonic energy into the reaction system. This breakthrough method not only broadens the application scope of CDs but also provides a novel pathway for the large-scale, high-efficiency production of high-performance CDs. In another study, Bi *et al.*[53] employed an

ultrasound-assisted, solvent-free method to synthesize antimicrobial carbon dots (LM-CDs) using PEG and liquid metals (LM) as precursors. These LM-CDs exhibited remarkable antibacterial activity against Gram-negative bacteria—including *E. coli*, *Pseudomonas aeruginosa* (*P. aeruginosa*), *Klebsiella pneumonia* (*K. pneumonia*), and *Acinetobacter baumannii*—as well as their antibiotic-resistant strains, with a minimum inhibitory concentration (MIC) as low as 0.63 μg mL^{-1}. The antibacterial mechanism of LM-CDs involves disruption of bacterial cell membranes, interference with iron metabolism, and generation of reactive oxygen species (ROS). Furthermore, animal studies confirmed that LM-CDs exhibit low biotoxicity and significantly accelerate wound healing, highlighting their potential for biomedical applications.

To facilitate a comprehensive comparison of various top-down synthesis techniques, Table 1 summarizes the characteristics, applicable material types, and technical advantages of several commonly used methods. The top-down methods for preparing antibacterial CNMs each exhibit distinct characteristics. For instance, laser ablation offers high precision and purity but comes at the cost of being energy-intensive and expensive. The arc discharge method, while particularly effective for producing CNTs with high crystallinity, is complex and requires substantial energy input. In contrast, electrochemical methods are notable for being environmentally friendly, cost-effective, and efficient, though there is a need for further improvements in QYs and purity. Ultrasonic synthesis, which is simple, non-toxic, and inexpensive, also faces challenges related to size control and yield consistency.[59,60] Overall, each preparation method possesses distinct advantages in terms of product properties, controllability, and economic feasibility. The choice of a method should be based on the specific requirements of the intended application.

2.2 Bottom-up synthesis methods

The bottom-up approach involves the synthesis of CNMs through the aggregation or chemical reactions of atoms, molecules, or smaller units. Compared to top-down methods, this approach is more effective in producing CNMs with uniform sizes and well-defined morphologies.[61]

2.2.1 Hydrothermal synthesis method. Among the various methods for synthesizing CQDs, the hydrothermal method stands out due to its simplicity, efficiency, and ability to produce uniformly sized particles with high QYs while requiring minimal equipment.[62] The synthesis process begins with dissolving a carbon source in water or an organic solvent mixture, which is then transferred into a high-pressure reactor. The reaction occurs under high-temperature and high-pressure conditions, typically lasting several hours. By precisely controlling parameters such as steam pressure, temperature, and reaction time, the size and morphology of the resulting CQDs can be effectively tailored. To further enhance surface properties and chemical stability, surfactants, carbon-based materials, or other functional additives are often introduced into the reaction system. These additives also facilitate the removal of strong alkaline substances, such as ammonia, improving the quality of the final product. The resulting CQDs exhibit high QYs and tuneable fluorescence emission properties, making them suitable for diverse applications, including bioimaging, sensing, and optoelectronics.[32]

The selection of carbon precursors plays a crucial role in hydrothermal synthesis. These precursors range from natural biomaterials, such as apple juice, hemicellulose, bamboo leaves, cabbage, and black tea, to waste materials, including discarded polytetrafluoroethylene (PTFE) from syringes and hyaluronic acid.[63–67] Under high-temperature and high-pressure conditions, these precursors undergo dehydration, polymerization, carbonization, and passivation, ultimately forming

Table 1 Common methods for the preparation of antimicrobial carbon nanomaterials *via* top-down approaches

Preparation method	Main features	Preparable nanostructures	Advantages	References
Laser ablation	High-energy laser pulses vaporize or decompose carbon materials, forming nanoscale particles	Carbon dots, carbon nanotubes, graphene quantum dots	High precision, high purity, good controllability	39 and 54
Electric arc discharge	A high current between graphite electrodes induces evaporation and re-condensation of carbon, forming nanostructures	Carbon nanotubes, carbon dots, graphene nanosheets	High efficiency, high product quality, simple equipment	55 and 56
Electrochemical method	Voltage applied to a carbon electrode in an electrolyte induces exfoliation, forming carbon nanostructures	Carbon dots, carbon nanotubes, graphene oxide	Environmentally friendly, efficient, easy to operate	46 and 57
Ultrasonic synthesis	Microbubbles generated by pressure waves collapse, creating shear forces that break down carbon materials into nanoscale sizes. Forces, breaking down large carbon-based materials into nanoscale sizes	Carbon dots, graphene quantum dots	Easy to operate, non-toxic	53 and 58

CQDs.[68,69] This approach underscores the economic, environmentally friendly, and non-toxic nature of hydrothermal synthesis by enabling the repurposing of waste materials.[70,71]

Significant progress has been made in utilizing hydrothermal synthesis to produce antibacterial CDs. For instance, Ghataty *et al.*[72] synthesized highly fluorescent bovine serum albumin (BSA)-derived carbon dots (B-CDs) using BSA as a precursor. These BCDs demonstrated strong antibacterial activity, effectively inhibiting the growth of various wound-infecting pathogens. Their antibacterial mechanism is likely associated with the presence of hydroxyl functional groups on the BCDs' surface, which disrupt the integrity of bacterial cell membranes. Similarly, Wei *et al.*[73] synthesized nitrogen-doped carbon dots (N-CDs) using folic acid and acetamide through hydrothermal synthesis. These N-CDs exhibited selective recognition and inhibition of various microorganisms, demonstrating particularly strong antibacterial effects against *E. coli*. Their antibacterial activity is attributed to disruption of bacterial cell membranes, which compromises bacterial viability. Ma *et al.*[74] employed a microwave-assisted glycolysis of polyethylene terephthalate (PET) waste, combined with hydrothermal synthesis, to prepare N-CDs. These N-CDs exhibited excellent fluorescence properties and broad-spectrum antibacterial activity against both Gram-positive and Gram-negative bacteria. Their antibacterial mechanism is primarily attributed to electrostatic interactions between the positively charged N-CDs surfaces and negatively charged bacterial cell membranes, ultimately leading to membrane rupture.

The hydrothermal synthesis method holds great promise for the production of antibacterial CDs. By carefully selecting carbon sources and doping elements, both antibacterial activity and fluorescence properties of CQDs can be tailored to meet specific application requirements. These antibacterial CDs exhibit significant potential in biomedicine, environmental protection, and water treatment. However, due to the high-temperature and high-pressure conditions involved in the process, strict safety measures must be implemented to ensure both effective and safety in large-scale applications.[68,75]

2.2.2 Microwave synthesis method. Microwave-assisted synthesis is an environmentally friendly and cost-effective method that enables the rapid and efficient production of CQDs.[49] This technique utilizes microwave radiation to rapidly heat the carbon precursor, triggering carbonization or pyrolysis reactions that lead to CQDs formation. The method is characterized by short reaction times, high yields, low energy consumption, and the potential for solvent-free synthesis, making it a sustainable alternative to conventional approaches.[32,76]

A key advantage of the microwave-assisted method is its compatibility with a wide range of carbon sources, including small organic molecules such as citric acid and urea, as well as natural biomaterials like orange peel powder and mango leaves.[77–79] For example, Lee *et al.*[77] synthesized nitrogen-doped CQDs with a high QY (22.26%) within 30 minutes using citric acid and urea as precursors. The resulting CQDs demonstrated excellent photostability and low cytotoxicity, making them particularly suitable for fluorescent labelling of bacterial cells. Similarly, Yalshetti *et al.*[80] utilized microwave-assisted synthesis with hibiscus leaf extract as a carbon source to produce CQDs exhibiting antibacterial, anti-inflammatory, and wound-healing properties, thereby expanding their potential for biomedical applications.

Furthermore, microwave-assisted synthesis holds great promise for the development of functional CQDs tailored for specific applications. By precisely controlling synthesis conditions, CQDs can be optimized for use in metal ion detection, bioimaging, and drug delivery.[68] For instance, Osman *et al.*[81] synthesized nitrogen and sulphur co-doped carbon quantum dots (N–S/CQDs) from alfalfa biomass using a microwave-assisted synthesis, which demonstrated high sensitivity for detecting nitrofurazone in pharmaceutical samples. This process not only ensures rapid synthesis but also aligns with the principles of green chemistry by being environmentally friendly and cost-effective. Despite the significant advancements achieved with microwave-assisted synthesis, challenges remain in precisely controlling the size and uniformity of the CQDs. Future research should focus on elucidating the underlying mechanisms of microwave-driven synthesis and optimizing reaction conditions to achieve greater precision in CQDs size control.

2.2.3 Template synthesis method. The template-assisted synthesis method utilizes the adsorption, reaction, or encapsulation properties of carrier materials to anchor carbon precursors onto the template surface. In this process, the carrier material acts as a structural template, guiding the morphology, size, and structural characteristics of the resulting CQDs. Following CQDs formation, the template is removed through high-temperature pyrolysis, solvent extraction, or acid/base etching. This method enables precise control over morphology, particle size, surface properties, and optoelectronic characteristics, making it particularly suitable for the synthesis of CQDs with tailored functionalities for specialized applications. However, template-assisted synthesis is often associated with complex and costly procedures, as well as challenges such as incomplete template removal, difficulties in separation and purification, and relatively low yields.[82] For example, Liu *et al.*[83] utilized F127-functionalized silica spheres as templates and phenolic resin as a carbon precursor to achieve the efficient synthesis of highly uniform CQDs with high water solubility and improved yields. By modifying the carbon precursor composition—such as incorporating resorcinol—they successfully synthesized multicolour photoluminescent CQDs, demonstrating the adaptability and tunability of this approach. Additionally, these CQDs exhibited good biocompatibility, making them highly suitable for high-resolution bioimaging applications. Similarly, Zong *et al.*[84] employed mesoporous silica microspheres as templates, loading citric acid as a carbon source, followed by pyrolysis and etching steps to synthesize CQDs with precisely controlled sizes of approximately 2 nm. These ultra-small CQDs exhibited excellent optical properties, rendering them highly suitable for advanced bioimaging applications.

Table 2 provides a comparative overview of the key characteristics, commonly used template materials, and advantages of various bottom-up synthesis methods. The bottom-up approach for the fabrication of antibacterial CNMs involves the spontaneous formation of nanostructures under controlled chemical

Table 2 Summary of common methods for the preparation of antimicrobial carbon nanomaterials *via* bottom-up methods

Preparation method	Main features	Prepared nanostructures	Advantages	References
Hydrothermal method	Precursors dissolved in water or organic solvents undergo high-temperature, high-pressure reactions	Carbon dots, graphene, carbon nanotubes	Cost-effective, highly controllable, non-toxic, environmentally friendly	85–87
Solvothermal method	High-temperature, high-pressure reactions in non-aqueous or organic solvents synthesize carbon nanomaterials	Carbon dots, graphene, porous carbon materials	Broad applicability, controllable conditions, cost-effective, eco-friendly	88–90
Microwave method	Microwave radiation uniformly heats organic matter, inducing carbonization for nanoscale carbon production	Carbon dots, graphene	High efficiency, controlled particle size, scalable, eco-friendly	91 and 92
Pyrolysis	Thermal decomposition of carbon sources in a vacuum or inert atmosphere	Carbon dots, graphene, carbon nanotubes, porous carbon materials	Cost-effective, versatile raw materials, flexible, easy operation	93–96
Carbonization	Organic materials decompose under high-temperature, anaerobic conditions to form carbon structures	Carbon dots, porous carbon materials	Cost-effective, free of harmful chemicals	97 and 98
Chemical vapor deposition	Gaseous precursors decompose at high temperatures, depositing carbon nanomaterials on a substrate	Carbon dots, graphene, carbon nanotubes	Scalable production, high quality, excellent controllability	99 and 100

reaction conditions. This method is highly versatile and adaptable, offering a wide range of applications. Among the various techniques, the hydrothermal and solvothermal methods are favoured for their environmental benefits, low cost, and tuneable reaction conditions. However, these methods present challenges in terms of controlling the size of the synthesized products and often require extended synthesis times. In contrast, microwave-assisted synthesis is efficient, scalable, and capable of producing high yields. However, it may be hindered by high energy consumption, which could result in increased operational costs. Pyrolysis and carbonization methods are simple, cost-effective, and compatible with a broad range of raw materials, but they require further optimization to achieve uniformity in product size and yield. The chemical vapor deposition method, while capable of producing high-quality CNMs, necessitates advanced equipment and incurs significant operational costs.[59,60] Overall, while the bottom-up approach enables the controllable synthesis of various carbon nanostructures with relatively lower energy consumption, further research is required to enhance size control and reduce production costs.

3. Structural properties of carbon nanomaterials and their antibacterial activity against Gram-negative bacteria

3.1 Graphene quantum dots

Graphene quantum dots are nanoscale fragments of graphene, typically measuring only a few nanometers in all three dimensions, classifying them as quasi-zero-dimensional materials.[101] GQDs integrate the exceptional physicochemical properties of graphene with the distinctive characteristics of quantum dots. Unlike bulk graphene, GQDs exhibit pronounced quantum confinement effects and surface defects, endowing them with unique optical and electronic properties, such as wavelength-dependent fluorescence emission, high photostability, excellent biocompatibility, and ease of conjugation with biological molecules.[102,103] These attributes render GQDs highly promising for a wide range of applications, including nonlinear optics, magnetic media, catalysis, pharmaceuticals, and functional materials.[104,105] Recent advancements have further highlighted the potential of GQDs in antimicrobial applications, particularly against Gram-negative bacteria.

The antibacterial activity of GQDs against Gram-negative bacteria underscores their potential as effective antimicrobial agents. One key factor influencing their antibacterial efficacy is functionalization, which enhances their physicochemical properties. Luo *et al.*[106] synthesized adenosine-functionalized graphene quantum dots (A-GQDs) *via* a two-step microwave-assisted method, yielding materials with strong fluorescence characteristics. Notably, A-GQDs exhibited remarkable biocompatibility and two-photon fluorescence for cell imaging. Under white light illumination, A-GQDs displayed selective antibacterial activity, showing no effect on *S. aureus* but almost completely inhibiting the growth of *E. coli*, demonstrating their specificity against Gram-negative bacteria.

Moreover, multi-element-doped GQDs have exhibited substantial antibacterial effects against Gram-negative bacteria. Huang *et al.*[107] developed halogen/nitrogen co-doped graphene quantum dots (X/N-PGQDs) as light-emitting diode-assisted bactericidal agents. These X/N-PGQDs demonstrated a MIC of less than 0.5 μg mL^{-1} against Gram-negative bacteria, indicating their potent antimicrobial efficacy. Additionally, GQDs-based composites have shown promise in combating Gram-negative bacteria. For instance, Yu *et al.*[108] successfully conjugated AgNPs onto the surface of GQDs, forming a GQDs-AgNPs composite with broad-spectrum antibacterial properties. Under 450 nm excitation, this composite exhibited significantly enhanced bactericidal activity against Gram-negative bacteria compared to GQDs alone.

Research further suggests that integrating GQDs with other functional materials can significantly improve their antibacterial efficacy. Yin *et al.*[109] synthesized GQDs using a bottom-up approach and combined them with alendronate (ALN) and AgNPs to create the composite material ALN-GQDs-Ag. This composite exhibited strong antibacterial activity against *Streptococcus mutans* biofilms, highlighting its potential for practical antimicrobial applications. Furthermore, the antibacterial performance of GQDs composites can be optimized by fine-tuning the GQDs-to-material ratio. For example, Yang *et al.*[110] synthesized a novel photocatalyst, GQDs/NH_2-MIL-125, using a solvothermal method. Their findings revealed that a 2% GQDs loading in the composite achieved 92% antibacterial activity against *E. coli*, underscoring the crucial role of GQDs concentration in optimizing antibacterial performance.

3.2 Carbon dots

Carbon dots are fluorescent carbon-based nanomaterials characterized by a core composed of sp^2-hybridized carbon atoms and a surface composed of sp^3-hybridized carbon atoms. These unique nanostructures exhibit exceptional electrical and chemical stability, low biotoxicity, environmental friendliness, and strong optical properties. Typically, CDs have a size of less than 10 nm, which enables them to closely resemble biological entities such as proteins, DNA, ion channels, and glomerular filtration barriers in the human body. Furthermore, the surface of CDs, depending on the synthesis method, is often functionalized with groups such as carboxyl, carbonyl, hydroxyl, and other functional moieties derived from precursor materials. These surface modifications contribute to their high-water solubility and biocompatibility.[111] Consequently, CDs are increasingly favored for various biomedical applications, including drug delivery, gene therapy, photosensitization, and antibacterial therapies.[112,113] Additionally, ongoing research continues to highlight their potential in multifunctional diagnostic platforms, cellular and bacterial bioimaging, and the advancement of nanomedicine.[114–116]

In recent years, there has been growing interest in the antibacterial activity of CDs. As research has progressed, the mechanisms underlying their antibacterial properties have become a primary focus. Early studies emphasized light-activated antibacterial properties, while more recent advancements have successfully overcome the limitations imposed by lightdependence. Moreover, strategies for functional modification are being explored to address the emerging issue of antibiotic resistance. This evolving field has made significant strides, as evidenced by the recent advances summarized in the timeline of antibacterial CDs research (Fig. 1).

A pioneering study on the visible and natural light-activated antibacterial properties of CDs demonstrated that ethylenediamine (EDA)-functionalized carbon quantum dots (EDA-CQDs) could effectively inhibit *E. coli* both in suspension and on agar surfaces under visible or natural light.[123] Experimental results revealed a significant reduction in bacterial colony counts on agar plates following treatment with light-activated EDA-CQDs, indicating a strong inhibitory effect on *E. coli* growth in culture media. Subsequently, Pandey *et al.*[124] synthesized antibacterial CDs that exhibited antimicrobial activity independent of light activation. Using citric acid as the carbon source and β-alanine as the surface passivating agent, they successfully produced CDs *via* microwave-assisted synthesis. Their findings

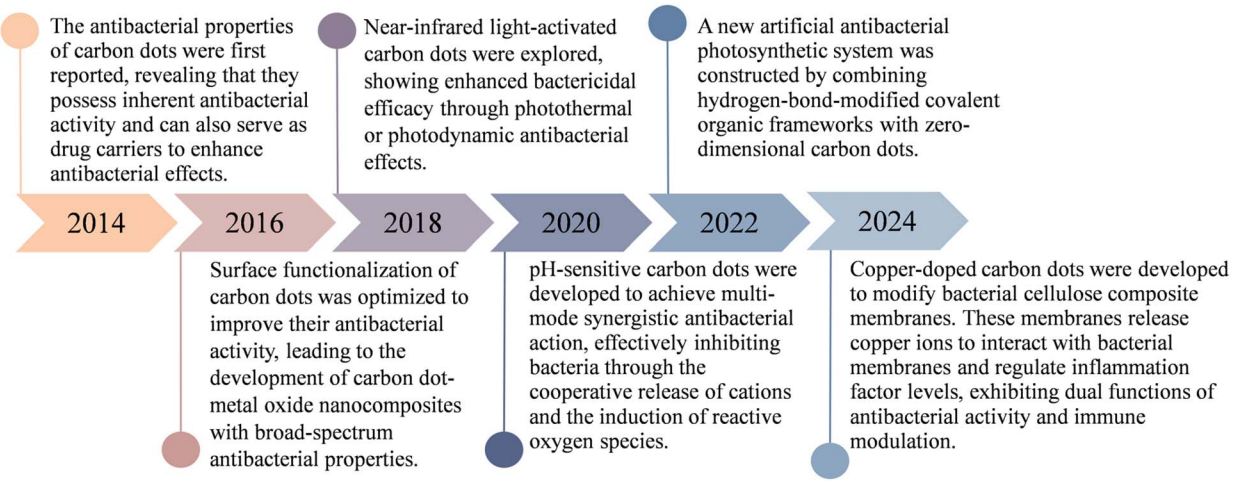

Fig. 1 Research progress on antibacterial carbon dots.[117–122]

Table 3 Effect of different functional groups on the antimicrobial properties of carbon dots

Type	Functional group formula	Antimicrobial mechanism	Antimicrobial effect	References
Quaternary ammonium group	$-NR_4^+$	Positively charged nitrogen interacts with negatively charged bacterial surfaces, disrupting membranes and causing cell death	Fast sterilization, most effective at pH ≥ 9	127 and 128
Quaternary phosphonate group	$-PR_4^+$	Larger ionic radii and stronger polarization of phosphorus enable better adsorption to bacterial surfaces	Broad applicability, effective in pH range 2–12	129 and 130
Guanidino group	$-C(=NH)NH_2$	Protonation of the guanidine group allows electrostatic interactions, rupturing bacterial membranes and leading to cell death	Highly effective against drug-resistant strains	131 and 132
N-Halamine group	–NX (X = Cl, Br)	Positively charged halogens transfer to bacterial receptors, inhibiting growth	Renewable, efficient, broad-spectrum sterilization	133 and 134

demonstrated that these CDs inhibited the growth of several Gram-negative bacterial strains, including *E. coli*, *Salmonella*, *Pseudomonas*, *Agrobacterium*, and *Pectinobacterium*. Notably, these CDs retained their antibacterial efficacy even after prolonged incubation in the absence of light, addressing the need for CDs with inherent antibacterial properties that do not rely on external light activation. Furthermore, unlike conventional antibiotics, these CDs exhibited a significantly lower tendency to induce bacterial resistance, offering a promising strategy to mitigate the global challenge of antibiotic resistance. Further advancing this field, Wu *et al.*[125] synthesized levofloxacin-functionalized carbon dots (L-CDs) using a simple one-pot hydrothermal method. These L-CDs exhibited potent antibacterial activity, with a MIC of 0.125 μg mL^{-1} against *E. coli*, and demonstrated strong inhibitory effects against antibiotic-resistant bacterial strains. Moreover, L-CDs displayed excellent biocompatibility both *in vitro* and *in vivo*, effectively overcoming the limitations associated with traditional antibiotics in clinical applications. The antibacterial properties of CDs can be attributed not only to their nanoscale size and unique surface chemistry but also to the presence of various functional groups introduced during synthesis. To enhance both antibacterial efficacy and biocompatibility, CDs must be functionalized with specific chemical groups. These modifications play a critical role in determining the primary antibacterial mechanisms, thereby optimizing their effectiveness.[126] Based on the distinct properties of different functional groups, researchers have developed a wide range of functionalized CDs to address the diverse challenges associated with combating Gram-negative bacterial infections. Table 3 provides a summary of the effects of various functional group modifications on the antibacterial performance of CDs.

3.3 Carbon nanotubes

Carbon nanotubes are one-dimensional nanomaterials composed of graphene sheets, where carbon atoms are arranged in a sp^2 hybridized structure. These sheets are coiled around a central axis at a specific helical angle, forming seamless, hollow tubes. Depending on the number of graphene sheets, CNTs can be classified as single-walled carbon nanotubes (SWCNTs) or multi-walled carbon nanotubes (MWCNTs). Due to their exceptional tensile strength, mechanical durability, large surface area, light-weight, chemical stability, superior transmembrane ability, and remarkable electronic, optical, and magnetic properties,[135–137] CNTs have significant potential for applications in drug delivery,[138] biosensors,[139] and tumour hyperthermia.[140] Furthermore, the discovery of their antibacterial activity has sparked growing interest in their use for environmental and human health applications.[141]

The antibacterial efficacy of CNTs, particularly against Gram-negative bacteria, is closely related to their physicochemical properties. The synthesis method significantly influences the types and concentrations of impurities in CNTs, which in turn affect their antibacterial performance. For example, Kang *et al.*[142] investigated the interactions between purified and raw SWCNTs and the model strain *E. coli* K12. Their results demonstrated that highly purified SWCNTs exhibited stronger antibacterial activity than raw CNTs. Additionally, factors such as surface area, dispersibility, and other physicochemical characteristics influence the antibacterial activity of CNTs. CNTs with better dispersibility and larger surface areas are more effective in interacting with bacteria, enhancing direct contact and uptake. For instance, SWCNTs, with smaller diameters and lengths compared to MWCNTs, offer a larger surface area, making them more efficient in inhibiting *E. coli* growth.[143] Functionalization plays a pivotal role in modulating the antibacterial properties of CNTs. Pasquini *et al.*[144] examined nine different functionalized SWCNTs and their interactions with *E. coli*. Their findings revealed that functionalization could indirectly influence the antibacterial activity of CNTs by altering their physicochemical properties, with the effects varying depending on the functional group applied. Additionally, combining CNTs with other materials to create composite

structures has proven to be an effective strategy for enhancing their antibacterial properties. For example, Khalil *et al.*[56] synthesized AgNPs-CNTs using an arc discharge method. These composites exhibited significantly enhanced antibacterial performance compared to individual AgNPs alone.

Furthermore, optimizing the loading ratio of metal nanoparticles in CNT-based composites is essential for maximizing antibacterial activity. Assis *et al.*[145] employed a microwave-assisted hydrothermal synthesis to load various concentrations (1, 5, and 10 wt%) of copper nanoparticles (CuNPs) onto MWCNTs. Their findings indicated that CNT-Cu 10, with a 10 wt% copper load, exhibited the highest antibacterial effect, with a MIC of 64 μg mL^{-1} against *E. coli*. Additionally, novel synthesis methods aimed at optimizing the structure and surface properties of CNTs have been shown to significantly improve their antibacterial performance. For instance, Yan *et al.*[146] used a sacrificial template method to prepare oxygen-modified nitrogen-doped CNTs (O-NCNTs-6), which demonstrated excellent antibacterial properties, achieving inactivation rates of 96% and 93% for *S. aureus* and *P. aeruginosa*, respectively, when tested on stainless steel electrodes in PBS. Furthermore, external factors, such as the dispersing medium, bacterial species, and the interaction method between CNTs and bacteria, can also impact the antibacterial activity of CNTs against Gram-negative bacteria.

3.4 Graphene

Graphene is a two-dimensional carbon nanomaterial composed of a single layer of carbon atoms bonded *via* sp^2 hybridization, forming a hexagonal crystal structure. It serves as the fundamental structural unit for other carbon allotropes, including fullerene (zero-dimensional), CNTs (one-dimensional), and graphite and diamond (three-dimensional). The thickness of a single graphene layer is approximately 0.35 nm, conferring exceptional stability and endowing the material with unique physical properties. These properties include outstanding thermal and mechanical performance, exceptional electronic conductivity, and remarkable optical characteristics.[147,148] Additionally, graphene possesses a high surface area, excellent catalytic activity, and notable antibacterial properties, rendering it highly suitable for applications across diverse fields, including electronics, information technology, energy, physics, biomedicine, and materials science.[149–151] Among these applications, graphene-based nanomaterials have garnered significant attention in the field of biomedicine. Graphene derivatives, such as GO, reduced graphene oxide (rGO), GQDs, and graphene-based nanocomposites, have been extensively explored for use in biosensors,[152,153] bioimaging,[154–156] drug delivery,[157,158] and photothermal therapy[159] among other applications. Furthermore, graphene nanomaterials have shown considerable promise as antimicrobial agents. To date, numerous studies have demonstrated the effective antibacterial activity of graphene-based nanomaterials against Gram-negative bacteria. The first reports on the antimicrobial properties of graphene nanomaterials specifically targeted Gram-negative bacteria. In 2010, Hu *et al.*[160] were the first to report the antibacterial properties of graphene, discovering that GO and rGO could inhibit *E. coli* growth by over 90%. Since then, research has expanded to include a variety of graphene composites engineered to target Gram-negative bacteria. For instance, Liu *et al.*[161] prepared GO coatings on polymer matrices and investigated their antibacterial activity against both *E. coli* and *S. aureus*. The results indicated that thinner GO coatings exhibited stronger antibacterial activity against *E. coli*, while thicker coatings were more effective against *S. aureus*. In another study, Matharu *et al.*[162] successfully fabricated antibacterial polymer nanocomposite fibers containing GO nanosheets using a pressure-assisted spinning method. These GO-based nanocomposites demonstrated significant antibacterial potential, with bacterial reduction rates ranging from 46% to 85%, and the nanocomposite containing 8% GO showing the highest biological activity. This highlights the importance of combining novel fabrication techniques with material composites to enhance the antibacterial performance of graphene-based nanomaterials. Thangaraj *et al.*[94] employed onion peel waste to prepare rGO through a one-step pyrolysis method. The study demonstrated that rGO-WiC, produced with the aid of a ferrocene catalyst, exhibited an inhibition zone of 566 mm^2 against *K. pneumoniae* at a concentration of 200 μg mL^{-1}, with the largest antibacterial effect observed against *E. coli* (inhibition zone area of 647 mm^2). Notably, the antibacterial activity of rGO-WiC was found to be 38.5% greater than that of rGO produced without a catalyst. Moreover, optimizing the structure and functionalization of composite materials has proven to be an effective strategy for enhancing the antibacterial properties of graphene-based nanomaterials. For example, Guo *et al.*[163] utilized GO as a template to develop a copper–iron sulfide nanocomposite (GO/$CuFeS_x$ NC) and tested various Cu/Fe ratios to identify the most effective antibacterial nanoenzyme combination. Under near-infrared (NIR) light stimulation, at a temperature of 45 °C, the GO/$Cu_3Fe_1S_x$ nanocomposite at a concentration of 40 μg mL^{-1}, combined with 100 μM hydrogen peroxide (H_2O_2), completely eradicated *E. coli*, demonstrating remarkable antibacterial activity.

4. Antimicrobial mechanism of carbon nanomaterials

The antibacterial efficacy of CNMs against Gram-negative bacteria is primarily attributed to their distinctive physicochemical properties, including specific morphology, size, and surface functionalization. Extensive research has elucidated several widely recognized antibacterial mechanisms, including physical disruption of bacterial membranes, oxidative stress induction, photothermal and photodynamic effects, lipid extraction, inhibition of bacterial energy metabolism, suppression of nucleic acid synthesis, DNA damage, bacterial encapsulation and isolation, and catalytic sterilization (Fig. 2).

4.1 Physical/mechanical disruption

CNMs of varying dimensionality can induce mechanical damage to bacterial outer membranes or cell walls, exhibiting

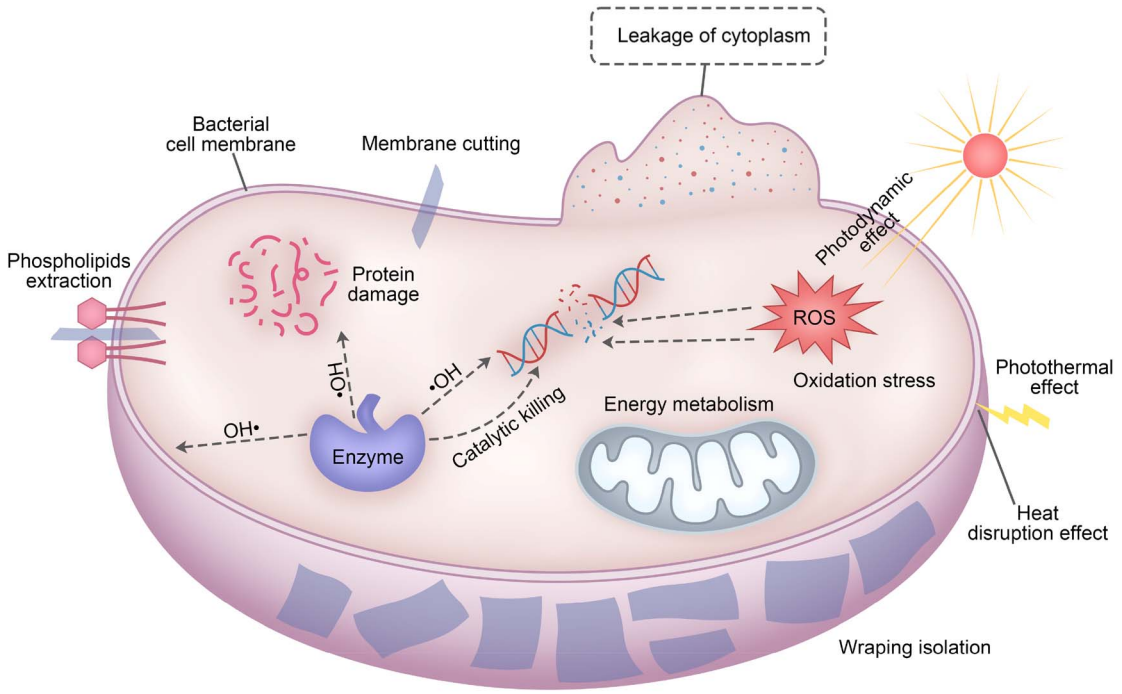

Fig. 2 Schematic representation of the antibacterial mechanism of CNMs.

both bactericidal and bacteriostatic effects. Zero-dimensional, one-dimensional, and two-dimensional CNMs interact with bacterial membranes in ways analogous to point, line, and planar interactions, respectively. The degree of mechanical disruption is closely associated with the nanomaterials' structural characteristics. Chatterjee *et al.*[164] demonstrated that carboxylated nanodiamonds, upon adhesion to the *E. coli* cell wall, altered the structural integrity of membrane proteins, ultimately leading to membrane rupture and bacterial cell death. Similarly, Wang *et al.*[165] synthesized CQDs from *Artemisia argyi* (A-CDs) using a simulated smoking method. Their findings revealed that A-CDs exhibited selective antibacterial activity by inhibiting enzyme functions essential for Gram-negative bacterial cell wall synthesis. Notably, A-CDs selectively compromised the cell walls of Gram-negative bacteria without affecting those of Gram-positive bacteria, highlighting their targeted specificity. Kang *et al.*[142,143] investigated the interaction between CNTs and bacteria, demonstrating that direct contact with CNTs induced morphological deformations, membrane disruption, intracellular leakage, and ultimately, bacterial cell death. These findings underscore the potent antibacterial properties of CNTs. For graphene materials (GMs), Wang *et al.*[166] employed molecular dynamics simulations to investigate graphene's cutting action, revealing that graphene sheets could disrupt phospholipid bilayers due to their sharp, sheet-like structures. Subsequent studies confirmed that when bacterial cells came into contact with GMs, the sharp edges of graphene sheets physically lacerated bacterial membranes, leading to cytoplasmic leakage and bacterial inactivation.[167] Furthermore, the orientation and angle of graphene sheets during contact significantly influenced their bactericidal efficiency. Shangguan *et al.*[168] reported that CDs synthesized from branched polyethylenimine (bPEI25000-CDs) exhibited notable antibacterial activity. Specifically, positively charged ALA-bPEI25000-CDs strongly interacted with bacterial cell membranes, leading to structural damage and cellular dysfunction. Scanning electron microscopy (SEM) images revealed that *E. coli* cells treated with these CDs displayed rough, deformed surfaces, ultimately resulting in membrane rupture. Similarly, Ruan *et al.*[169] synthesized N–S/CQDs, which exhibited broad-spectrum antibacterial activity. This activity was closely linked to their nanoscale size, surface functional groups, and the ability to generate ROS. Mechanical disruption was identified as a key antibacterial mechanism, with N–S/CQDs effectively penetrating bacterial membranes, inducing structural damage, and inhibiting bacterial proliferation. The incorporation of amine functional groups conferred a positive charge to the N–S/CQDs, enhancing electrostatic interactions with negatively charged bacterial membranes, and thereby improving antibacterial efficacy. By fine-tuning the surface properties and dimensions of N–S/CQDs, their antibacterial performance was further optimized, offering new strategies for developing advanced antimicrobial nanomaterials. Zhao *et al.*[170] observed pronounced morphological changes in *S. aureus* cells treated with vancomycin–malic acid–amines carbon dots (VMA-CDs), including pore formation and membrane rupture, indicating severe bacterial damage. These findings confirmed that VMA-CDs exert their antibacterial effects by disrupting bacterial membrane integrity. Furthermore, Wang *et al.*[171] synthesized CDs from ornidazole *via* microwave radiation and investigated their selective antibacterial mechanisms against *Porphyromonas gingivalis* (*P. gingivalis*). The study

revealed that CDs with specific molecular weights (1–10 kDa) exhibited strong antibacterial effects against *P. gingivalis*, while having minimal impact on *Streptococcus mutans*. This selectivity was attributed to the nanoscale dimensions of the CDs, which facilitated membrane penetration, membrane integrity disruption, and the release of antibacterial functional groups, such as nitro groups, effectively eliminating the target bacteria. Li *et al.*[172] showed that carbon dots with specific surface functional groups could cause significant morphological changes in bacterial cells. Their study revealed that the positively charged carbon dots could strongly interact with bacterial cell membranes, leading to structural damage and cellular dysfunction. Scanning electron microscopy (SEM) images indicated rough and deformed surfaces of *E. coli* cells treated with these carbon dots, ultimately resulting in membrane rupture and cell death. Furthermore, it was observed that carbon dots with amine functional groups could enhance electrostatic interactions with negatively charged bacterial membranes, thereby improving antibacterial efficacy. By adjusting the surface properties and dimensions of carbon dots, their antibacterial performance could be further optimized, providing new strategies for developing advanced antimicrobial nanomaterials. Mortimer *et al.*[173] indicated that CNTs cause mechanical damage to bacterial cells through direct contact, leading to membrane rupture and cytoplasmic leakage. The physical properties of carbon nanomaterials, such as their sharp edges and high surface area, enable them to interact closely with bacterial cell membranes and exert physical disruption effects. This not only damages the bacterial cell membrane but also compromises the integrity of the cell wall, thereby enhancing the antibacterial efficacy of carbon-based nanomaterials.

4.2 Oxidation stress

The induction of oxidative stress by CNMs is widely recognized as an effective antibacterial mechanism. This process disrupts the oxidant–antioxidant balance within bacterial cells, leading to cellular damage. Oxidative stress can occur through two primary pathways: ROS-dependent and ROS-independent mechanisms. The ROS-dependent pathway is initiated by the excessive accumulation of intracellular ROS, such as superoxide anions ($^{\bullet}O_2^-$), hydrogen peroxide, hydroxyl radicals ($^{\bullet}OH$), and singlet oxygen. Numerous studies have demonstrated that elevated ROS levels can cause protein inactivation, lipid peroxidation, mitochondrial dysfunction, and membrane degradation, ultimately resulting in bacterial necrosis or apoptosis.[174] In contrast, ROS-independent oxidative stress refers to the damage or oxidation of essential cellular structures or intracellular components without the direct involvement of ROS. This pathway represents an alternative oxidative stress response that does not rely on ROS generation. For instance, graphene and its derivatives can induce oxidative stress by oxidizing intracellular glutathione, thereby increasing ROS levels and promotes the oxidation of fatty acids. This oxidation leads to the formation of lipid peroxides, triggering free radical reactions, resulting in the destruction and lysis of biological membranes and induce bacterial cell death. Gurunathan *et al.*[175] in their investigation of the antibacterial properties of graphene against *P. aeruginosa*, reported a 3.8-fold and 2.7-fold increase in intracellular ROS levels in bacteria treated with GO and rGO, respectively. These findings confirm that graphene exerts its antibacterial effects *via* ROS-dependent oxidative stress. Similarly, other studies have proposed that oxidative stress is a key mechanism underlying the antibacterial properties of CNTs.[143] Vecitis *et al.*[176] demonstrated that the interaction between MWCNTs and *E. coli* led to an increase in glutathione oxidation within bacterial cells. The degree of oxidation was directly proportional to the concentration of metallic SWNTs, indicating that enhanced oxidative stress was responsible for the observed antibacterial activity. This suggests that CNTs interfere with bacterial metabolism through oxidative stress, leading to intracellular dysfunction and effective bacterial inhibition. Further research by Bing *et al.*[177] explored the effects of CDs on *E. coli* growth and their underlying antibacterial mechanisms. The study revealed significant variations in ROS levels induced by three types of CQDs (S-CQDs, C-CQDs, and G-CQDs), indicating that endogenous ROS levels play a crucial role in triggering bacterial apoptosis and determining the antibacterial efficacy of these nanomaterials. Recent studies have provided deeper insights into the oxidative stress mechanism of carbon dots. Cui *et al.*[178] demonstrated that spermidine-capped carbon dots (S-PCDs) could effectively induce intracellular ROS generation in *Staphylococcus aureus*. Their experiments showed that S–P/CDs, at a concentration equal to the MIC, elevated ROS production to 5.25-fold that of the control group. As the S–P/CDs concentration increased, ROS levels rose further, reaching 6.52-fold the control at four times the MIC. The study revealed that S–P CDs, with their high positive charge (+47.06 mV), could adsorb onto the negatively charged bacterial surface *via* electrostatic interactions. This interaction not only facilitated the generation of ROS but also induced significant oxidative stress, leading to cell membrane damage and eventual bacterial cell death. The ROS generation pathways were found to involve the activation of oxidative stress-related genes such as dmpI, narJ, and narK. The upregulation of these genes promoted increased oxidative stress through non-photonic pathways within the bacterial cells, further exacerbating membrane damage and cell death. Similarly, Rosato *et al.*[179] found that GQDs exposed to blue light exhibited significantly enhanced antibacterial activity against *E. coli*. In their study, GQDs were administered to *E. coli* suspensions and treated with blue light. The results showed that blue light stimulation enhanced GQDs' antibacterial activity in a time-dependent manner attributed to ROS production by GQDs under blue light irradiation. Sun *et al.*[180] discovered that CDs can efficiently generate ROS under irradiation, which can disrupt bacterial cell membranes and proteins. They found that nitrogen-doped CDs exhibited higher ROS generation efficiency when stimulated by blue light, resulting in stronger antibacterial effects. The study also highlighted the importance of CD-bacterial cell envelope interactions in the antibacterial process. CDs can specifically target and bind to bacterial cell surfaces, enhancing ROS generation and improving antibacterial efficacy. Recently, Xia

et al.[181] prepared nitrogen-doped carbon quantum dots to inactivate antibiotic resistant bacteria through spontaneous generation of extracellular and intracellular ROS, which was supported by the significant regulation of genes related to oxidative stress.

4.3 Photothermal effect

Under NIR irradiation, CNMs exhibit exceptional photothermal conversion efficiency, rendering them highly effective in antibacterial applications. Various photothermal CNMs have been developed, characterized by strong NIR absorption and the ability to efficiently convert light energy into heat. The localized heat generation can effectively inhibit bacterial growth and prevent biofilm formation. In 2007, Kim *et al.*[182] utilized *E. coli* as a model organism to explore the potential of CNTs in photothermal antibacterial therapy. This study was among the first to propose that CNMs exert antibacterial effects *via* photothermal mechanisms. The findings demonstrated that CNTs could self-assemble into clusters on bacterial surfaces and exhibit responsiveness to NIR laser stimulation. Upon NIR excitation, CNTs generated localized high temperatures, significantly reducing *E. coli* viability.

Beyond CNTs, other CNMs, such as GO and rGO, also exhibit photothermal antibacterial properties. However, rGO demonstrates superior photothermal antibacterial efficiency compared to GO, primarily due to its higher intrinsic thermal conductivity and enhanced NIR absorption. Tan *et al.*[183] investigated the antibacterial activity of rGO/Ag nanocomposites against *E. coli* and *K. pneumoniae*. Their results indicated that rGO/Ag nanocomposites exhibited enhanced synergistic antibacterial activity through photothermal effects. Under NIR irradiation, these nanocomposites not only generated heat but also induced membrane disruption and ROS production, thereby significantly improving antibacterial efficacy.

Additionally, in the case of CDs, modifying the core structure through transition metal doping or forming composites with metal nanoparticles has been identified as an effective strategy to enhance their photothermal antibacterial performance.[184]

4.4 Photodynamic effect

The principle of photodynamic therapy (PDT) was first discovered by Oscar Raab in Munich in 1900 through a serendipitous observation. PDT is based on three essential components: oxygen, a photosensitizer, and visible light (typically laser light). Upon irradiation with light of a specific wavelength, the photosensitizer becomes excited, initiating a photochemical reaction. The photosensitizer transfers energy to surrounding oxygen molecules, resulting in the generation of highly reactive singlet oxygen. This singlet oxygen subsequently interacts with nearby biological macromolecules through oxidative reactions, leading to cytotoxicity and ultimately bacterial cell death. CNMs have demonstrated efficacy as photosensitizers in PDT, exhibiting antibacterial activity through the light-dependent generation of ROS. Ristic *et al.*[185] synthesized GQDs *via* electrochemical reactions and observed ROS production upon light excitation. These GQDs exhibited inhibitory effects against methicillin-resistant *Staphylococcus aureus* (MRSA) and *E. coli*, confirming their potential as PDT agents for antibacterial applications. In 2016, Kuo *et al.*[186] utilized nitrogen-doped graphene quantum dots (N-GQDs) as photosensitizers to eliminate *E. coli* through PDT. Their findings revealed that GQDs with higher nitrogen doping levels (5.1%) exhibited significantly enhanced PDT effects and antibacterial activity compared to those with lower nitrogen content (2.9%). Building upon this, Kuo *et al.*[187] further synthesized nitrogen-doped, amine-functionalized graphene quantum dots (AN-GQDs). These AN-GQDs demonstrated a higher capacity for ROS generation compared to unmodified GQDs, effectively combating multidrug-resistant bacteria through PDT. Zühlke *et al.*[188] explored the use of amorphous carbon nanodots (CNDs) for photodynamic sterilization. By controlling the irradiation wavelength to exceed 290 nm, they minimized damage to bacterial outer membranes while enhancing immune responses. Due to their small particle size, CNDs were able to penetrate bacterial membranes and generate ROS internally under ultraviolet (UV) light, thus accelerating bacterial inactivation. Experimental results showed that photodynamic inactivation using UV light in conjunction with CNDs was ten times more effective than UV treatment alone. Bacterial membrane integrity was further confirmed through aggregation studies and atomic force microscopy (AFM). In a study by Kadyan *et al.*[189] the unique properties of GQDs under UV and visible light irradiation were investigated. The results indicated that nitrogen-doped GQDs acted as efficient photosensitizers, generating various ROS, including H_2O_2, $^{\bullet}OH$, $^{\bullet}O_2^-$, and singlet oxygen. These ROS interacted with water and dissolved oxygen (O_2), inducing oxidative stress within bacterial cells and leading to cytotoxic effects and bacterial death. Rosato *et al.*[179] demonstrated that CNMs like GQDs exhibit excellent photothermal conversion efficiency under NIR irradiation, inhibiting bacterial growth and biofilm formation. Temperature increases enhanced bacterial membrane permeability, facilitating antimicrobial agent penetration. Simultaneously, the photodynamic effect of CNMs can generate ROS under light irradiation. For example, GQDs and CDs produce singlet oxygen and superoxide anions under specific wavelengths of light, which have strong oxidizing properties, causing oxidative damage to bacterial cells.

4.5 Phospholipids extraction

CNMs can also interact with bacterial cells through lipid extraction mechanisms. Bacterial membranes, particularly those of Gram-negative bacteria, are composed of both an outer and an inner lipid bilayer, which are essential for functions such as nutrient uptake and the expulsion of toxic substances. Disruption of the structural and functional integrity of these membranes results in bacterial inhibition or cell death.[190] In contrast to mechanical damage, which physically disrupts the bacterial cell wall or outer membrane, CNMs with abundant surface-active sites can penetrate the bacterial lipid bilayers. This penetration facilitates the extraction of phospholipids from the lipid bilayer onto the surface of the nanomaterials,

thereby compromising membrane integrity and ultimately leading to bacterial death. In 2013, Tu *et al.*[191] conducted both experimental and theoretical studies to elucidate the lipid extraction effect of GO nanosheets on bacterial membranes. Their findings revealed that GO nanosheets disrupted the bacterial membrane by directly extracting significant quantities of phospholipid molecules, leading to bacterial death. Molecular dynamics simulations further demonstrated that the two-dimensional planar structure of GO interacts with phospholipids through van der Waals forces and strong hydrophobic interactions, facilitating the adsorption of phospholipids onto the GO surface. Liu and Yi *et al.*[192,193] further confirmed GO–phospholipid bilayer interactions, noting that lipid extraction is size-dependent, with larger GO sheets exhibiting stronger effects. Other studies identified lipid extraction as a primary mechanism for CNT-induced lipid bilayer damage.[194]

4.6 Inhibition of bacterial energy metabolism

Bacteria rely on metabolic processes to convert nutrients into energy and to eliminate metabolic waste, essential for growth and survival. Unlike eukaryotic cells, bacteria lack mitochondria. ATPases involved in energy metabolism are embedded in the bacterial cell membrane. Many antibacterial agents exert their effects by inhibiting the synthesis of peptidoglycan (PG), a critical component of the bacterial cell wall, thereby disrupting bacterial energy metabolism. Recent studies show that CNMs can induce bacterial cell death by suppressing energy metabolism. Mashino *et al.*[195] reported that fullerene derivatives accept electrons from the bacterial respiratory chain, reacting with oxygen to generate H_2O_2. This reaction inhibits oxygen uptake in the *E. coli* respiratory chain, suggesting that antibacterial activity of fullerene derivatives is mediated by the disruption of bacterial energy metabolism. In addition, the ability of GQDs to inhibit PG synthesis has been extensively studied. Xin *et al.*[28] demonstrated that D-glutamic acid-functionalized GQDs (DGGs) can penetrate bacterial cell membranes and specifically target MurD ligase, an enzyme critical for PG biosynthesis. By inhibiting MurD's catalytic activity, DGGs disrupt cell wall synthesis, leading to membrane damage, cytoplasmic leakage, and ultimately bacterial death. DGGs exhibited high antibacterial activity and selective toxicity *in vitro*. In contrast, unmodified GQDs and L-glutamic acid-functionalized GQDs, although capable of penetrating bacterial membranes, showed weaker interactions with MurD ligase and did not exhibit significant antibacterial activity.

4.7 Inhibition of nucleic acid synthesis and DNA damage

To effectively inhibit bacterial growth and reproduction at the molecular level, various antibacterial agents have been developed that target nucleic acid synthesis and DNA damage mechanisms. In the context of CNMs, it has been demonstrated that these materials can directly interact with DNA, thereby exerting antibacterial effects. Wu *et al.*[196] demonstrated that GO can form complexes with DNA through coordination interactions, which protect the DNA from enzymatic degradation. However, in the presence of copper ions, GO can disrupt the DNA structure, leading to damage.[197] Subsequent studies have confirmed that CNMs exhibit antibacterial activity by inhibiting nucleic acid synthesis, binding to DNA molecules, impeding DNA replication, and inducing DNA damage. Li *et al.*[46] synthesized positively charged CQDs using a one-step electrochemical method with vitamin C as the precursor. These CQDs exhibited broad-spectrum antibacterial activity. Experimental results revealed that the positively charged CQDs were capable of diffusing into bacterial cells, disrupting the cell wall, and non-covalently binding to bacterial DNA and RNA. This interaction resulted in the loosening of the DNA structure, leading to the unwinding of the double helix, fragmentation of the genetic material, and subsequent cell inactivation, ultimately resulting in bacterial cell death even at very low concentrations. Moreover, studies have shown that spermidine-functionalized carbon quantum dots (Spd-CQDs), which exhibit a high positive surface charge (zeta potential of up to 60.6 mV), can interact multivalently with negatively charged bacterial membranes. This interaction causes severe cytoplasmic damage and leakage. Notably, at low concentrations, Spd-CQDs can bind to nucleic acids such as plasmid DNA and small interfering RNA (siRNA), disrupting gene expression regulation and exerting antibacterial effects.[198] Nangan *et al.*[67] synthesized fluorescent carbon dots (S-CDs) *via* a hydrothermal method using waste PTFE from discarded syringes as the precursor material. These S-CDs exhibited significant antibacterial activity by adhering to bacterial cell walls, penetrating the membrane, and binding to DNA. This interaction led to DNA unwinding, compromising bacterial structural integrity, and enhancing antibacterial efficacy. Furthermore, Yao *et al.*[199] highlighted that quantum dots can damage DNA either through their intrinsic nanoscale morphology or *via* the release of metal ions. Their antibacterial activity is also attributed to the generation of ROS and the inhibition of DNA damage repair mechanisms.

4.8 Wrapping isolation

In addition to the previously discussed antibacterial mechanisms, certain CNMs with large surface areas can inhibit bacterial proliferation by enveloping the bacteria, thereby isolating them from their environment. Researchers have found that GMs, with their hexagonal two-dimensional crystal structure, can act as a physical barrier, effectively separating bacteria from their surroundings and preventing the proliferation of Gram-negative bacteria. Although encapsulated bacteria retain their original shape, the separation from the external environment restricts the exchange of substances and information between bacterial cells. This disruption reduces their intracellular metabolic activity and vitality, ultimately inhibiting bacterial growth. Furthermore, the encapsulation effect of GMs can also induce damage to the bacterial cell membrane.[200] Chen *et al.*[201] proposed that GO exerts its antibacterial effects by wrapping and entangling microorganisms, which leads to depolarization of the bacterial cell membrane or electrolyte leakage. Furthermore, it was observed that graphene nanoplatelets (GNPs) larger than 5.2 nm can adhere to bacterial membranes due to the strong hydrophobic interactions between graphene and the lipid bilayer. Larger and better-dispersed GO nanoplatelets can more efficiently envelop

bacteria, blocking active sites on the bacterial membrane, thereby inhibiting bacterial growth and reducing their survival potential.[202] Studies on the antibacterial properties of CNTs have also demonstrated a similar encapsulation effect. Chen *et al.*[203] confirmed that the antibacterial mechanism of CNTs is associated with both diameter-dependent perforation and length-dependent encapsulation of bacterial cell walls and membranes. Longer MWCNTs, by increasing the contact area with the bacterial cell wall, are more likely to encapsulate bacteria, thereby exhibiting enhanced antibacterial activity.

4.9 Catalytic sterilization

Certain CNMs have been found to exhibit enzyme-like catalytic activities, enabling the conversion of H_2O_2 into highly reactive $^{\bullet}OH$. As a potent oxidizing agent, $^{\bullet}OH$ induces oxidative stress responses that disrupt bacterial cell membranes, inactivate proteins, and cause DNA damage, ultimately interfering with bacterial growth and metabolic processes. This catalysis-based antibacterial mechanism presents new opportunities for the application of CNMs in antimicrobial research. Qi *et al.*[204] synthesized iron-doped carbon dot nanozymes (Fe-CDs) using *Eucommia ulmoides* (a traditional Chinese medicinal herb) as a biomass-derived carbon source *via* a hydrothermal method. The peroxidase-like (POD) activity of Fe-CDs was confirmed by monitoring the oxidation of 3,3′,5,5′-tetramethylbenzidine (TMB). Furthermore, when Fe-CDs were combined with H_2O_2, a significant reduction in the characteristic absorption intensity of methylene blue (MB) at 665 nm was observed, further verifying their ability to catalyze the conversion of H_2O_2 into $^{\bullet}OH$. Antibacterial experiments demonstrated that the combination of Fe-CDs and H_2O_2 produced a significantly larger inhibition zone compared to either agent alone, achieving a bactericidal rate of 94.82%. In another study, Wang *et al.*[205] developed copper-doped carbon dots (Cu-CDs) with exceptional POD activity using cherry blossom biomass *via* a hydrothermal process. UV-vis spectroscopy was employed to evaluate the oxidation capacity of different CDs on TMB solutions. The results demonstrated that Cu-CDs efficiently catalyzed the decomposition of H_2O_2 into $^{\bullet}OH$, achieving bactericidal rates exceeding 90% against both *E. coli* and *S. aureus*. These findings underscore the potent catalytic activity of metal-doped CDs in antimicrobial applications. Additionally, Zhang *et al.*[206] engineered multifunctional glucose oxidase/carbon dots@copper metal–organic framework nanofibers (GOx/CDs@MOF NFs). Their study revealed that glucose oxidase (GOx) catalyzed the conversion of physiological glucose into gluconic acid and H_2O_2, concurrently lowering the pH of the system. This acidic environment effectively enhanced the POD activity of the Cu-MOF, further validating the potential of CNMs to improve antibacterial efficacy through catalytic mechanisms.

5. Antimicrobial applications of carbon nanomaterials in medicine

In summary, CNMs, due to their remarkable antibacterial properties, hold significant promise in the field of medical antibacterial applications. Their potential is increasingly recognized across a wide range of medical domains, including oral health, antimicrobial dressings, tissue engineering, medical sutures, pneumonia treatments, and urinary catheters. As research in this area progresses, these materials are expected to play an increasingly pivotal role in combating bacterial infections, providing innovative solutions for both infection prevention and treatment within clinical settings.

5.1 Dentistry

In dental medicine, *P. gingivalis*, a non-glycolytic, Gram-negative anaerobic bacterium, is a primary pathogen responsible for periodontitis. CDs have emerged as promising antibacterial agents, interacting with the negatively charged surface structures of *P. gingivalis via* their positively charged surfaces. This interaction aids in controlling infections and contributes to the treatment of dental caries and periodontal diseases. Liu *et al.*[207] were the first to investigate the antibacterial effects of fluorescent CDs on *P. gingivalis*, an obligate anaerobe commonly found in the oral cavity. Using metronidazole as a precursor, they synthesized fluorescent CDs *via* a one-step hydrothermal method. Their findings revealed that at a concentration of 1.25 μg mL^{-1}, the fluorescent CDs achieved an inhibition rate of 71.7% against *P. gingivalis*, with the antibacterial effect increasing proportionally with higher concentrations of CDs. This discovery holds considerable promise for the diagnosis, treatment, and prevention of dental caries and periodontal diseases, paving the way in further exploration into the application of fluorescent CDs for targeting oral bacteria. Liang *et al.*[208] successfully synthesized therapeutic CQDs (T-CQDs and M-CQDs) using sulfonyl metronidazole and metronidazole as precursors through a hydrothermal process. These CQDs demonstrated strong inhibitory effects against *P. gingivalis*, with TCDs exhibiting the additional ability to penetrate bacterial biofilms, enhancing their efficacy in suppressing the growth of *P. gingivalis*. This advancement represents a novel strategy for improving periodontitis treatment outcomes, offering new therapeutic options for managing oral bacterial infections.

5.2 Antibacterial accessories

In the field of biomedical materials, the development of biomaterials with antimicrobial properties plays a critical role in medical applications, particularly in preventing microbial infections associated with medical devices and wound care. Recent studies have demonstrated the potential of polymer-functionalized CNTs as effective antimicrobial agents for use in biomedical coatings and wound dressings. Simmons *et al.*[209] fabricated SWCNTs coatings functionalized with polyvinylpyrrolidone-iodine (PVP-I), which exhibited significant antibacterial activity against *E. coli*. When incorporated into conductive nanofiber bandages, these materials demonstrated excellent flexibility and antimicrobial efficacy, effectively reducing bacterial colonization at wound sites and accelerating the healing process. Furthermore, CNTs functionalized with amino acids such as arginine and lysine, as well as those

modified with antimicrobial peptides, have shown exceptional antibacterial performance, underscoring their potential for development as advanced antimicrobial biomaterials.[210–212] Beyond CNTs, other CNMs have also exhibited promising antibacterial capabilities. For instance, Wang *et al.*[213] developed an antibacterial composite film by incorporating lanthanum-doped nitrogen and phosphorus co-doped carbon quantum dots (La@N–P-CQDs) into a polyvinyl alcohol (PVA) matrix. This composite film achieved an inhibition rate exceeding 99% against *E. coli*. In addition to its strong antibacterial properties, the PVA/La@N–P-CQDs composite film exhibited excellent hydrophilicity, biocompatibility, and fluorescence intensity, making it a multifunctional material with potential applications in biomedical settings. Notably, *in vivo* studies demonstrated its ability to significantly enhance wound healing, highlighting its potential as an effective antimicrobial adjunct in clinical medicine.

5.3 Tissue engineering

Infectious bone defects present a significant challenge in the treatment of orthopedic infectious diseases, particularly those resulting from severe open fractures caused by high-impact trauma. These injuries are often accompanied by varying degrees of wound contamination, extensive soft tissue damage, compromised blood supply, and substantial bone loss. As a result, there is an urgent need for the development of bone graft materials that not only possess robust antibacterial properties but also enable controlled drug release and demonstrate excellent osteogenic activity, thereby addressing both infection and bone defect repair following open fractures.[214] Graphene-based nanocomposites have shown considerable promise in promoting the growth of human and mammalian cells, positioning them as potential candidates for use as scaffolding materials in tissue engineering applications. Mazaheri *et al.*[215] fabricated graphene oxide–chitosan (GO–CS) composites as antibacterial scaffolds to support stem cell proliferation. Similarly, Faghihi *et al.*[216] employed GO nanosheets as reinforcing agents in polyacrylic acid/gelatin composite hydrogels, creating antibacterial scaffolds with enhanced suitability for tissue engineering applications. Building on these advancements, Weng *et al.*[217] incorporated antibiotics into graphene-based three-dimensional composite scaffolds, creating localized, controlled-release systems that combine both bone-filling and antibacterial functions. This innovative strategy leverages the superior properties of graphene to enhance local drug concentrations while minimizing systemic side effects, offering a promising solution for treating infectious bone defects associated with open fractures.

5.4 Medical sutures

Medical sutures play a critical role in wound closure by approximating tissue edges, stabilizing the wound, and facilitating natural healing. To minimize adverse reactions, suture materials must exhibit excellent biocompatibility and biodegradability. However, despite advancements in sterile techniques, suture materials remain susceptible to microbial adhesion, potentially leading to post-surgical infections. Therefore, the ideal suture material should possess intrinsic antibacterial properties to mitigate the risk of infection. Recent advancements in nanotechnology have highlighted the potential of carbon-based nanomaterials, such as graphene and CNTs, in enhancing the antibacterial properties of sutures, thereby improving wound infection control. For instance, Ma *et al.*[218] incorporated mechanically exfoliated graphene into a PVA matrix to fabricate PVA/GO nanocomposite fibres using gel spinning and stretching techniques. While PVA fibres alone lack antibacterial properties, the incorporation of GO significantly enhanced the antimicrobial activity of the composite fibres. In wound healing experiments, nanocomposite fibres containing 0.3 wt% GO exhibited a marked reduction in healing time compared to conventional surgical sutures, suggesting their potential as a novel alternative for surgical applications. In another study, de Moura *et al.*[219] developed two antibacterial nanocomposites by combining GNPs and MWCNTs with a poly(lactic acid) (PLA) and thermoplastic polyurethane (TPU) blend at a 60/40 ratio. The resulting composites, designated as 60/40/GNP_2 and 60/40/MWCNTs/GNP_1, demonstrated significant antibacterial activity in agar diffusion assays, with distinct inhibition zones, indicating their efficacy in preventing bacterial colonization. Furthermore, recent research suggests that integrating natural polymers with GO could provide an effective strategy for developing next-generation antimicrobial suture materials. Gayathri *et al.*[220] fabricated suture materials using cellulose, chitosan (CS), and GO. Their agar diffusion and simulated body fluid (SBF) studies confirmed that these sutures exhibited strong antibacterial activity, particularly against *E. coli*, further underscoring their potential as advanced antimicrobial suture materials.

5.5 Pneumonia

Bacterial pneumonia remains a prevalent respiratory infection in modern medicine, with its treatment increasingly complicated by the rise of multidrug-resistant bacterial strains.[221] The widespread use of antibiotics has contributed to the development and dissemination of resistant pathogens, posing a significant threat to global public health. Consequently, traditional antibiotic therapies are often ineffective against these resistant bacteria, highlighting the urgent need for novel antimicrobial strategies and materials. Serrano-Aroca *et al.*[222] identified carbon-based nanomaterials as promising candidates for the treatment of bacterial pneumonia. These materials exhibit potent antibacterial activity primarily through physical mechanisms, such as disruption of bacterial cell walls and the generation of ROS. Such mechanisms are particularly valuable for targeting pneumonia-causing pathogens, offering substantial clinical potential. Notably, carbon nanomaterials can impair bacterial cell wall integrity and disrupt biofilm structures, thus increasing bacterial susceptibility to antibiotics. This characteristic is especially significant for treating biofilm-associated pneumonia infections, which are often more resistant to conventional therapies. Furthermore, the biocompatibility and low toxicity of carbon nanomaterials make them

highly attractive for clinical applications. For instance, combining carbon nanomaterials with antibiotics has been shown to enhance antibacterial efficacy, particularly against drug-resistant bacterial strains responsible for pneumonia. Research conducted by Wu *et al.*[223] supports these findings, demonstrating that carbon nanomaterials have promising effects in controlling pneumonia infections caused by resistant bacteria. When used in conjunction with antibiotics, carbon nanomaterials significantly improve treatment outcomes. These results suggest that carbon nanomaterials can serve both as standalone therapeutic agents and as adjuncts to traditional antibiotics, offering a synergistic effect that enhances treatment efficacy against resistant pathogens. This interaction not only improves overall treatment effectiveness but also provides a valuable complement to conventional antibiotics, introducing a novel approach to combating bacterial pneumonia. Despite these promising results, clinical data remain limited, and large-scale clinical trials are essential to further assess the safety and efficacy of carbon nanomaterials in real-world medical settings.

5.6 Medical catheter

Catheter-associated urinary tract infections (CAUTIs) represent a major category of hospital-acquired infections, accounting for approximately 40% of such cases. These infections significantly impact patients' quality of life and pose considerable risks to their health and safety. Consequently, enhancing the antibacterial properties of urinary catheters is of paramount clinical importance for the prevention of urinary tract infections. CNMs, including CNTs, graphene-based materials, and CDs, possess unique physicochemical properties and inherent antibacterial activity, positioning them as promising candidates for the development of antimicrobial catheters. Zhang *et al.*[224] demonstrated that CNMs exhibit robust antibacterial properties with a reduced propensity for inducing bacterial resistance, contributing to their growing use in antimicrobial applications. In particular, the integration of CNMs into medical catheters has shown considerable potential, as these materials can disrupt bacterial outer membranes through both physical and chemical interactions, thereby slowing the development of microbial resistance. The distinctive properties of CNMs make them invaluable for the design of antibacterial composite materials, with significant promise for reducing the incidence of CAUTIs. Teixeira-Santos *et al.*[225] further explored the potential of nitrogen-functionalized graphene composites for urinary catheter applications. Their study revealed that nitrogen-functionalized graphene nanoplatelets (N-GNPs), when incorporated into a polydimethylsiloxane (PDMS) matrix to form N-GNP/PDMS composites, significantly inhibited the formation of both single-species and multi-species biofilms, particularly against *S. aureus*. Compared to pure PDMS, the N-GNP/PDMS composite exhibited increased surface roughness and hydrophobicity, which effectively reduced the colonization of *S. aureus*, *P. aeruginosa*, and *K. pneumoniae*, while also diminishing *S. aureus* biofilm formation. In multi-species biofilms, a reduction in total cell counts was also observed. Furthermore, N-GNPs were found to alter membrane permeability in *S. aureus* and promote the generation of ROS, while primarily affecting cellular metabolism in Gram-negative bacteria. Overall, the N-GNP/PDMS composite demonstrated significant potential as a urinary catheter coating material by effectively inhibiting biofilm development. Given the escalating issue of antibiotic resistance, the development of novel antimicrobial materials is becoming increasingly critical. The discovery of N-GNP/PDMS composites provides a promising direction for the design of urinary catheters and could play a pivotal role in reducing the risk of catheter-associated infections.

6. The toxicity about antibacterial CNMs

6.1 Toxicity assessment and metabolism of CNMs

The increasing applications of carbon nanomaterials in biomedicine necessitate a comprehensive understanding of their toxicity profiles. Li *et al.*[226] indicated those various carbon-based nanomaterials, including carbon black nanoparticles, nanodiamonds, fullerenes, and graphene quantum dots, exhibit diverse toxicological behaviours depending on their physicochemical properties. Researchers employ a range of *in vitro* and *in vivo* assays to evaluate their cytotoxic effects, encompassing MTT assays, flow cytometry, and confocal microscopy, which provide insights into cell viability, cell cycle progression, apoptosis, and autophagy. Comparative analyses between different carbon nanomaterials reveal that dimensionality significantly influences toxicity. For instance, Raja *et al.*[227] discovered that zero-dimensional carbon dots demonstrate dose-dependent cytotoxicity in human lung epithelial cells (A549), with IC50 values ranging from 200 to 500 μg mL^{-1}, whereas one-dimensional carbon nanotubes exhibit distinct biological interactions. These disparities underscore the importance of considering material dimensions in toxicity assessments. Furthermore, surface functionalization emerges as a critical determinant of biocompatibility. Ecological risk assessments further refine safety thresholds, with Kim *et al.*[228] proposing 10 μg L^{-1} as an environmental safety limit for aquatic systems based on *Daphnia magna* immobilization tests.

CNMs usually have high biological stability, which makes them relatively difficult to degrade *in vivo*.[229] CNMs typically exhibit high biological stability, making them relatively difficult to degrade *in vivo*. Although there is currently a lack of direct research in the metabolic behaviour of CNMs against Gram negative bacteria, the *in vivo* metabolism or distribution of biological CNMs continues to attract significant interest. Kim *et al.*[228] quantified this concern through comparative pharmacokinetic studies, revealing that carbon nanotubes exhibit 30% slower clearance rates than gold nanoparticles in murine models. Correspondingly, researchers are trying to overcome non-biodegradability and stability challenges. Surface modification and functionalization strategies effectively address biodegradability limitations. Li *et al.*[226] demonstrated that carboxyl group incorporation enhances both water dispersibility and enzymatic degradation of carbon nanotubes, significantly reducing accumulation risks. Chen *et al.*[230]

developed poly(amidoamine) dendrimer-crosslinked nanotubes that maintain antimicrobial efficacy while improving colloidal stability. Emerging research directions focus on intrinsically biodegradable designs that retain antimicrobial activity.

6.2 Balancing efficacy and biosafety

While carbon nanomaterials effectively combat Gram-negative bacteria *via* membrane disruption and oxidative stress pathways, their potential cytotoxicity toward eukaryotic cells requires meticulous evaluation. Nasirzadeh *et al.*[231] observed a 60% viability loss in HEK293 kidney cells at 50 μg mL^{-1} pristine graphene oxide exposure, attributing this toxicity to lysosomal membrane destabilization. This finding underscores the urgency of developing targeted antimicrobial strategies. Advanced material design approaches demonstrate promising solutions to this biosafety challenge. Li *et al.*[226] engineered sulfur-doped reduced graphene oxide nanosheets that achieved a 5-log reduction in *Pseudomonas aeruginosa* at 120 μg mL^{-1} while maintaining 92% viability in L929 fibroblasts. Chiou *et al.*[232] and Zhang *et al.*[233] designed and prepared biomass-derived CNMs with excellent antibacterial activities and balanced the enhanced biocompatibility and reduced hemolysis at antimicrobial concentrations several times higher than the effective dose. Thus, the preparation of CNMs from biomass or the surface bioactivity modification are important strategies to improve both antibacterial and biosafety properties of CNMs.

7. Summary and outlook

The emergence of multidrug-resistant (MDR) and extensively drug-resistant (XDR) bacteria has made the development of new antimicrobial agents an urgent priority. Gram-negative bacteria, due to their unique biological structure, have long posed significant challenges in the development of effective antimicrobial agents. Unfortunately, in recent years, the field of antimicrobial drug development targeting Gram-negative bacteria has remained largely confined to existing classes of antibiotics. There remains a notable scarcity of new antimicrobial agents with novel mechanisms of action in clinical development. Carbon nanomaterials, with their inherent antimicrobial activity and distinctive physical antibacterial properties, offer new promise in an era characterized by widespread antibiotic misuse. If effectively applied in infection treatment, these materials may provide an innovative approach to combating bacterial resistance. However, several unresolved issues remain regarding the clinical application of carbon nanomaterials in antibacterial therapy. These challenges and development directions include: (1) the potential toxicity assessment of CNMs on human cells and tissues is incomplete. It is necessary to clarify the structure of CNMs and their interactions with biological targets, as well as their antibacterial molecular mechanisms. Furthermore, by precisely controlling parameters such as material size, shape, and surface chemical properties, and developing purification and large-scale preparation methods, some CNMs with tuneable antibacterial activity and minimal toxicity can be achieved. (2) There is insufficient understanding of the precise localization of CNMs in bacteria, cells, and organisms, and it is necessary to conduct safety evaluations and *in vivo* distribution research on antibacterial CNMs. Animal models and evaluation indicators need to be further studied for *in vivo* safety research to understand the *in vivo* long-term safety and stability of CNMs *in vivo*. The imaging, *in vivo* metabolism, and pharmacokinetics study methods of CNMs are needed to determine the optimal dosage regimen. (3) There is still a lack of consistency in the structure and properties of carbon dots across different production batches. Quality control standards, safety standards, usage strategies, and specialized guidelines and regulations need to be developed as a regulatory framework for fair use of antibacterial CNMs. (4) The combination of CNMs with other antibacterial drugs. For example, deepening the combination strategy of CNMs with traditional antibiotics, antimicrobial peptides, *etc.*, and enhancing antibacterial effects, reducing bacterial resistance risks, and improving biosafety.

Despite ongoing debates about the mechanisms underlying the antimicrobial activity of carbon nanomaterials, their potential applications in the antimicrobial field remain highly promising. As our understanding of the key functional parameters required for effective bacterial targeting at the molecular level deepens, continued efforts to optimize the design of carbon nanomaterials are expected. Moreover, advancing the exploration of their antimicrobial mechanisms will contribute to significant breakthroughs in both basic research and technological applications. In conclusion, this rapidly developing field has already achieved notable progress. We are optimistic that further exploration of the antimicrobial properties of carbon nanomaterials will accelerate the development of new agents against Gram-negative and resistant bacteria. In the near future, carbon nanomaterials are poised to play a key role in the clinical treatment of infections caused by Gram-negative and resistant bacteria.

Data availability

No primary research results, software or code have been included and no new data were generated or analysed as part of this review.

Author contributions

Chengwei Zhang, Ying Zheng, and Xiaoyan Lin: data curation, writing – original draft, writing – review & editing. Shaohuang Weng: conceptualization, supervision, project administration, writing – review &editing.

Conflicts of interest

There are no conflicts to declare.

Acknowledgements

The authors thank the financial support from the Joint Funds for the Innovation of Science and Technology, Fujian Province (2021Y9007), and the National Science Foundation of Fujian Province (2022J01493).

Notes and references

1 C. A. Bradley, *Nat. Rev. Drug Discovery*, 2018, **17**, 394.
2 Z. Wang, H. Zhang, J. Han, H. Xing, M. C. Wu and T. Yang, *Infect. Control Hosp. Epidemiol.*, 2017, **38**, 758–759.
3 G. V. Asokan and A. Vanitha, *Perspect. Public Health*, 2018, **138**, 87–88.
4 A. Upadhayay, J. Ling, D. Pal, Y. Xie, F. F. Ping and A. Kumar, *Drug Resistance Updates*, 2023, **66**, 100890.
5 Z. Breijyeh, B. Jubeh and R. Karaman, *Molecules*, 2020, **25**, 1340.
6 G. M. Carlone, M. J. Valadez and M. J. Pickett, *J. Clin. Microbiol.*, 1982, **16**, 1157–1159.
7 Y. Fujiwara, K. Ohnishi, H. Horlad, Y. Saito, D. Shiraishi, H. Takeya, D. Yoshii, S. Kaieda, T. Hoshino and Y. Komohara, *Clin. Transl. Immunol.*, 2020, **9**, e1162.
8 G. Mamou, F. Corona, R. Cohen-Khait, N. G. Housden, V. Yeung, D. Sun, P. Sridhar, M. Pazos, T. J. Knowles and C. Kleanthous, *Nature*, 2022, **606**, 953–959.
9 P. R. Murray, K. S. Rosenthal and M. A. Pfaller, *Medical Microbiology*, Elsevier Health Sci., 2020.
10 M. C. Sousa, *Nature*, 2019, **576**, 389–390.
11 S. I. Miller, *mBio*, 2016, **7**, DOI: **10.1128/mbio.01541-16**.
12 V. Gupta and P. Datta, *Indian J. Med. Res.*, 2019, **149**, 97–106.
13 M. Exner, S. Bhattacharya, B. Christiansen, J. Gebel, P. Goroncy-Bermes, P. Hartemann, P. Heeg, C. Ilschner, A. Kramer and E. Larson, *GMS Hyg Infect. Control*, 2017, **12**, Doc05.
14 M. Bassetti, A. Vena, C. Sepulcri, D. R. Giacobbe and M. Peghin, *Antibiotics*, 2020, **9**, 632.
15 E. Massa, E. Michailidou, D. Agapakis, S. Papadopoulos, T. Tholioti, I. Aleuroudis, T. Bargiota, M. Passakiotou, M. Daoudaki and N. Antoniadis, *Transplant. Proc.*, 2019, **51**, 454–456.
16 J. Chen, S. M. Andler, J. M. Goddard, S. R. Nugen and V. M. Rotello, *Chem. Soc. Rev.*, 2017, **46**, 1272–1283.
17 M. H. Kollef and K. D. Betthauser, *Curr. Opin. Infect. Dis.*, 2019, **32**, 169–175.
18 Y. Liu, W. Wang, H. Yan, D. Wang, M. Zhang and S. Sun, *Future Microbiol.*, 2019, **14**, 899–915.
19 S. Ghosh, S. Sen, M. Jash, S. Ghosh, A. Jana, R. Roy, N. Mukherjee, D. Mukherjee, J. Sarkar and S. Ghosh, *ACS Infect. Dis.*, 2024, **10**, 1267–1285.
20 H. Douafer, V. Andrieu, O. Phanstiel IV and J. M. Brunel, *J. Med. Chem.*, 2019, **62**, 8665–8681.
21 X. Gao, J. Ding, C. Liao, J. Xu, X. Liu and W. Lu, *Adv. Drug Delivery Rev.*, 2021, **179**, 114008.
22 A. Adak, S. Ghosh, V. Gupta and S. Ghosh, *Biomacromolecules*, 2019, **20**, 1889–1898.
23 A. Adak, V. Castelletto, B. Mendes, G. Barrett, J. Seitsonen and I. W. Hamley, *ACS Appl. Bio Mater.*, 2024, **7**, 5553–5565.
24 A. Adak, V. Castelletto, A. de Sousa, K. A. Karatzas, C. Wilkinson, N. Khunti, J. Seitsonen and I. W. Hamley, *Biomacromolecules*, 2024, **25**, 1205–1213.
25 R. Samat, S. Sen, M. Jash, S. Ghosh, S. Garg, J. Sarkar and S. Ghosh, *ACS Infect. Dis.*, 2024, **10**, 3098–3125.
26 S. Sen, R. Samat, M. Jash, S. Ghosh, R. Roy, N. Mukherjee, S. Ghosh, J. Sarkar and S. Ghosh, *J. Med. Chem.*, 2023, **66**, 11555–11572.
27 M. Hamad, F. Al-Marzooq, G. Orive and T. H. Al-Tel, *Drug Discovery Today*, 2019, **24**, 2225–2228.
28 Q. Xin, Q. Liu, L. Geng, Q. Fang and J. R. Gong, *Adv. Healthcare Mater.*, 2017, **6**, 1601011.
29 R. Van Noorden, *Nature*, 2011, **469**, 14.
30 D. Nagarajan, D. Gangadharan and S. Venkatanarasimhan, *Carbon Dots in Analytical Chemistry*, Elsevier, 2023, pp. 1–13.
31 J. Xu, B. Huang, C. M. Lai, Y. S. Lu and J. W. Shao, *J. Photochem. Photobiol., B*, 2024, **255**, 112920.
32 J. Kong, Y. Wei, F. Zhou, L. Shi, S. Zhao, M. Wan and X. Zhang, *Molecules*, 2024, **29**, 2002.
33 S. Paveethra, H. Manisekaran and S. Sasidharan, *Asian Pac. J. Cancer Prev.*, 2024, **25**, 3393.
34 Y. P. Sun, B. Zhou, Y. Lin, W. Wang, K. S. Fernando, P. Pathak, M. J. Meziani, B. A. Harruff, X. Wang and H. Wang, *J. Am. Chem. Soc.*, 2006, **128**, 7756–7757.
35 S. Santiago, T. N. Lin, C. H. Chang, Y. A. Wong, C. A. J. Lin, C. T. Yuan and J. Shen, *Phys. Chem. Chem. Phys.*, 2017, **19**, 22395–22400.
36 V. Nguyen, L. Yan, J. Si and X. Hou, *J. Appl. Phys.*, 2015, **117**, 084304.
37 L. Cui, X. Ren, J. Wang and M. Sun, *Mater. Today Nano*, 2020, **12**, 100091.
38 V. Nguyen, N. Zhao, L. Yan, P. Zhong and P. H. Le, *Mater. Res. Express*, 2020, **7**, 015606.
39 A. Menazea and M. Ahmed, *Nano-Struct. Nano-Objects*, 2020, **22**, 100464.
40 K. S. Khashan, G. M. Sulaiman and R. Mahdi, *Artif. Cells, Nanomed., Biotechnol.*, 2017, **45**, 1699–1709.
41 X. Xu, R. Ray, Y. Gu, H. J. Ploehn, L. Gearheart, K. Raker and W. A. Scrivens, *J. Am. Chem. Soc.*, 2004, **126**, 12736–12737.
42 F. Chao-Mujica, L. Garcia-Hernández, S. Camacho-López, M. Camacho-López, M. Camacho-López, D. Reyes Contreras, A. Pérez-Rodríguez, J. Peña-Caravaca, A. Páez-Rodríguez and J. Darias-Gonzalez, *J. Appl. Phys.*, 2021, **129**, 163301.
43 Y. Lin, M. Zhou, X. Tai, H. Li, X. Han and J. Yu, *Matter*, 2021, **4**, 2309–2339.
44 J. Ge, M. Lan, B. Zhou, W. Liu, L. Guo, H. Wang, Q. Jia, G. Niu, X. Huang and H. Zhou, *Nat. Commun.*, 2014, **5**, 4596.
45 P. G. Luo, F. Yang, S. T. Yang, S. K. Sonkar, L. Yang, J. J. Broglie, Y. Liu and Y. P. Sun, *RSC Adv.*, 2014, **4**, 10791–10807.
46 H. Li, J. Huang, Y. Song, M. Zhang, H. Wang, F. Lu, H. Huang, Y. Liu, X. Dai and Z. Gu, *ACS Appl. Mater. Interfaces*, 2018, **10**, 26936–26946.

47 X. Liu, L. Yu, F. Liu, L. Sheng, K. An, H. Chen and X. Zhao, *J. Mater. Sci.*, 2012, **47**, 6086–6094.
48 B. D. Mansuriya and Z. Altintas, *Nanomaterials*, 2021, **11**, 2525.
49 L. Cui, X. Ren, M. Sun, H. Liu and L. Xia, *Nanomaterials*, 2021, **11**, 3419.
50 S. Zhuo, M. Shao and S. T. Lee, *ACS Nano*, 2012, **6**, 1059–1064.
51 H. Huang, Y. Cui, M. Liu, J. Chen, Q. Wan, Y. Wen, F. Deng, N. Zhou, X. Zhang and Y. Wei, *J. Colloid Interface Sci.*, 2018, **532**, 767–773.
52 Y. Wu, Y. Liu, J. Yin, H. Li and J. Huang, *Talanta*, 2019, **205**, 120121.
53 S. Bi, C. Hang, J. Qi, W. Zhang and X. Jiang, *Adv. Biol.*, 2023, **7**, 2200297.
54 M. Al-Salih, S. Samsudin and S. S. Arshad, *J. Genet. Eng. Biotechnol.*, 2021, **19**, 76.
55 A. Barhoum, A. Meftahi, M. S. Kashef Sabery, M. E. Momeni Heravi and F. Alem, *J. Mater. Sci.*, 2023, **58**, 13531–13579.
56 A. M. Khalil, M. A. Gharieb, S. M. Abdelaty and A. M. El-Khatib, *Mater. Res. Express*, 2024, **11**, 075006.
57 F. Fenniche, A. Henni, Y. Khane, D. Aouf, N. Harfouche, S. Bensalem, D. Zerrouki and H. Belkhalfa, *J. Inorg. Organomet. Polym. Mater.*, 2022, **32**, 1011–1025.
58 F. Karkeh-Abadi, F. Soofivand, H. Safardoust-Hojaghan, Q. A. Yousif and M. Salavati-Niasari, *J. Mater. Res. Technol.*, 2022, **18**, 4413–4426.
59 N. H. Hussen, A. H. Hasan, Y. M. FaqiKhedr, A. Bogoyavlenskiy, A. R. Bhat and J. Jamalis, *ACS Omega*, 2024, **9**, 9849–9864.
60 S. Ross, R. S. Wu, S. C. Wei, G. M. Ross and H. T. Chang, *J. Food Drug Anal.*, 2020, **28**, 677.
61 P. D. Modi, V. N. Mehta, V. S. Prajapati, S. Patel and J. V. Rohit, *Carbon Dots in Analytical Chemistry*, Elsevier, 2023, pp. 15–29.
62 S. Pandiyan, L. Arumugam, S. P. Srirengan, R. Pitchan, P. Sevugan, K. Kannan, G. Pitchan, T. A. Hegde and V. Gandhirajan, *ACS Omega*, 2020, **5**, 30363–30372.
63 Z. Liang, L. Zeng, X. Cao, Q. Wang, X. Wang and R. Sun, *J. Mater. Chem. C*, 2014, **2**, 9760–9766.
64 A. M. Alam, B. Y. Park, Z. K. Ghouri, M. Park and H. Y. Kim, *Green Chem.*, 2015, **17**, 3791–3797.
65 J. Briscoe, A. Marinovic, M. Sevilla, S. Dunn and M. Titirici, *Angew. Chem., Int. Ed.*, 2015, **54**, 4463–4468.
66 S. Min, P. Ezati, K. S. Yoon and J. W. Rhim, *Int. J. Biol. Macromol.*, 2023, **231**, 123493.
67 S. Nangan, K. Kanagaraj, G. Kaarthikeyan, A. Kumar, M. Ubaidullah, B. Pandit, R. Govindasamy and T. Natesan, *Environ. Res.*, 2023, **237**, 116990.
68 G. Arora, N. S. Sabran, C. Y. Ng, F. W. Low and H. Jun, *Heliyon*, 2024, **10**, e35543.
69 P. C. Hsu and H. T. Chang, *Chem. Commun.*, 2012, **48**, 3984–3986.
70 S. Liu, J. Tian, L. Wang, Y. Zhang, X. Qin, Y. Luo, A. M. Asiri, A. O. Al-Youbi and X. Sun, *Adv. Mater.*, 2012, **24**, 2037.
71 S. Sahana, A. Gautam, R. Singh and S. Chandel, *Nat. Prod. Bioprospect.*, 2023, **13**, 51.
72 D. S. Ghataty, R. I. Amer, M. A. Amer, M. F. Abdel Rahman and R. N. Shamma, *Pharmaceutics*, 2023, **15**, 234.
73 S. Wei, X. Shi, C. Wang, H. Zhang, C. Jiang, G. Sun and C. Jiang, *Spectrochim. Acta, Part A*, 2023, **287**, 122039.
74 G. Ma, R. Wang, M. Zhang, Z. Dong, A. Zhang, M. Qu, L. Gao, Y. Wei and J. Wei, *Spectrochim. Acta, Part A*, 2023, **289**, 122178.
75 J. Peng, W. Gao, B. K. Gupta, Z. Liu, R. Romero-Aburto, L. Ge, L. Song, L. B. Alemany, X. Zhan and G. Gao, *Nano Lett.*, 2012, **12**, 844–849.
76 G. Magdy, H. Elmansi, M. M. Samaha, E. Said and N. El-Enany, *Sustainable Chem. Pharm.*, 2024, **37**, 101424.
77 S. J. Lee, Y. Y. Zheng, W. M. Chen and Y. H. Hsueh, *ACS Omega*, 2024, **9**, 36453–36463.
78 M. K. Kumawat, M. Thakur, R. B. Gurung and R. Srivastava, *ACS Sustainable Chem. Eng.*, 2017, **5**, 1382–1391.
79 P. M. Olmos-Moya, S. Velazquez-Martinez, C. Pineda-Arellano, J. R. Rangel-Mendez and L. F. Chazaro-Ruiz, *Carbon*, 2022, **187**, 216–229.
80 S. Yalshetti, B. Thokchom, S. M. Bhavi, S. R. Singh, S. R. Patil, B. Harini, M. Sillanpää, J. Manjunatha, B. Srinath and R. B. Yarajarla, *Sci. Rep.*, 2024, **14**, 9915.
81 M. M. Osman, R. El-Shaheny and F. A. Ibrahim, *Anal. Chim. Acta*, 2024, **1319**, 342946.
82 G. Ge, L. Li, D. Wang, M. Chen, Z. Zeng, W. Xiong, X. Wu and C. Guo, *J. Mater. Chem. B*, 2021, **9**, 6553–6575.
83 R. Liu, D. Wu, S. Liu, K. Koynov, W. Knoll and Q. Li, *Angew. Chem., Int. Ed.*, 2009, **48**, 4598–4601.
84 J. Zong, Y. Zhu, X. Yang, J. Shen and C. Li, *Chem. Commun.*, 2011, **47**, 764–766.
85 J. Lv, H. Tian, L. Pan, Z. Chen, M. Li, R. A. Ghiladi, Z. Qin and X. Yin, *Chem. Eng. Sci.*, 2024, **295**, 120084.
86 Y. Zhao, X. Wu, S. Sun, L. Ma, L. Zhang and H. Lin, *Carbon*, 2017, **124**, 342–347.
87 C. Shuai, X. Shi, K. Wang, Y. Gu, F. Yang and P. Feng, *Bio-Des. Manuf.*, 2024, **7**, 105–120.
88 B. Khan, J. Zhang, S. Durrani, H. Wang, A. Nawaz, F. Durrani, Y. Ye, F. G. Wu and F. Lin, *ACS Appl. Mater. Interfaces*, 2024, **16**, 47257–47269.
89 T. J. Antony and K. Jagannathan, *Ceram. Int.*, 2024, **50**, 16343–16351.
90 M. Zhang, H. Yang, K. Yang, Q. Yang, W. Liu and X. Yang, *J. Chromatogr. A*, 2024, **1725**, 464926.
91 Y. Liu, C. Huang, W. Yue, X. Wang, Y. Sun, W. Bi, L. Wang and Y. Xu, *Carbon*, 2024, **224**, 119085.
92 P. Kodithuwakku, D. Jayasundara, I. Munaweera, R. Jayasinghe, T. Thoradeniya, A. Bogahawatta, K. J. Manuda, M. Weerasekera and N. Kottegoda, *ACS Omega*, 2024, **9**, 26568–26581.
93 Z. Li, M. Zhou, L. Zhao, W. Hu, X. Wang, H. Wei, X. Tong, C. Yao, X. Li and Y. Zhang, *Chem. Eng. J.*, 2024, **498**, 155081.
94 B. Thangaraj, N. Wongyao, P. R. Solomon, V. Gupta, A. Abdullah, S. Abedrabbo and J. Hassan, *J. Environ. Chem. Eng.*, 2024, **12**, 113474.
95 S. He, J. Huang, Q. Zhang, W. Zhao, Z. Xu and W. Zhang, *Adv. Funct. Mater.*, 2021, **31**, 2105198.

96 Y. Bai, C. Shi, X. Ma, J. Li, S. Chen, N. Guo, X. Yu, C. Yang and Z. Zhang, *Chem. Eng. J.*, 2022, **447**, 137545.
97 R. Elizabeth Roy, N. KS, S. Salim, S. Sugathan and A. John, *Chem. Biodiversity*, 2025, **22**, e202401350.
98 R. Venkatesan, P. Sivaprakash, I. Kim, G. E. Eldesoky and S. C. Kim, *J. Environ. Chem. Eng.*, 2023, **11**, 110194.
99 J. Luan, W. L. Duan, Y. X. Li, F. B. Meng, Y. Liu, X. S. Zhang, J. Zhou, W. Z. Li and Y. Fu, *ACS Sustain. Chem. Eng.*, 2023, **11**, 12423–12434.
100 B. Yang, L. Gao, M. Xue, H. Wang, Y. Hou, Y. Luo, H. Xiao, H. Hu, C. Cui and H. Wang, *Materials*, 2021, **14**, 7356.
101 S. Kim, Y. Song and M. J. Heller, *Adv. Mater.*, 2017, **29**, 1701845.
102 S. N. Khan, B. M. Weight, B. J. Gifford, S. Tretiak and A. Bishop, *J. Phys. Chem. Lett.*, 2022, **13**, 5801–5807.
103 E. Haque, J. Kim, V. Malgras, K. R. Reddy, A. C. Ward, J. You, Y. Bando, M. S. A. Hossain and Y. Yamauchi, *Small Methods*, 2018, **2**, 1800050.
104 A. Ghaffarkhah, E. Hosseini, M. Kamkar, A. A. Sehat, S. Dordanihaghighi, A. Allahbakhsh, C. van der Kuur and M. Arjmand, *Small*, 2022, **18**, 2102683.
105 C. Zhao, X. Song, Y. Liu, Y. Fu, L. Ye, N. Wang, F. Wang, L. Li, M. Mohammadniaei and M. Zhang, *J. Nanobiotechnol.*, 2020, **18**, 1–32.
106 Z. Luo, D. Yang, C. Yang, X. Wu, Y. Hu, Y. Zhang, L. Yuwen, E. K. L. Yeow, L. Weng and W. Huang, *Appl. Surf. Sci.*, 2018, **434**, 155–162.
107 H. H. Huang, A. Anand, C. J. Lin, H. J. Lin, Y. W. Lin, S. G. Harroun and C. C. Huang, *Carbon*, 2021, **174**, 710–722.
108 Y. Yu, L. Mei, Y. Shi, X. Zhang, K. Cheng, F. Cao, L. Zhang, J. Xu, X. Li and Z. Xu, *J. Mater. Chem. B*, 2020, **8**, 1371–1382.
109 I. X. Yin, J. Y. Niu, M. L. Mei, J. Tang, W. K. K. Wu and C. H. Chu, *Int. J. Nanomed.*, 2024, **19**, 11195–11212.
110 G. Yang, L. Wang, C. Zhang, P. Li, H. Du, Y. Mao, M. Qiu, Q. Li, D. Hao and Q. Wang, *Sep. Purif. Technol.*, 2023, **312**, 123433.
111 X. Tian, A. Zeng, Z. Liu, C. Zheng, Y. Wei, P. Yang, M. Zhang, F. Yang and F. Xie, *Int. J. Nanomed.*, 2020, **15**, 6519–6529.
112 W. Q. Li, Z. Wang, S. Hao, L. Sun, M. Nisic, G. Cheng, C. Zhu, Y. Wan, L. Ha and S. Y. Zheng, *Nanoscale*, 2018, **10**, 3744–3752.
113 W. Su, R. Guo, F. Yuan, Y. Li, X. Li, Y. Zhang, S. Zhou and L. Fan, *J. Phys. Chem. Lett.*, 2020, **11**, 1357–1363.
114 M. Hassan, V. G. Gomes, A. Dehghani and S. M. Ardekani, *Nano Res.*, 2018, **11**, 1–41.
115 P. Devi, S. Saini and K.-H. Kim, *Biosens. Bioelectron.*, 2019, **141**, 111158.
116 Y. Bai, Y. Wang, L. Cao, Y. Jiang, Y. Li, H. Zou, L. Zhan and C. Huang, *Anal. Chem.*, 2021, **93**, 16466–16473.
117 A. S. Krishna, C. Radhakumary, M. Antony and K. Sreenivasan, *J. Mater. Chem. B*, 2014, **2**, 8626–8632.
118 K. Wang, Q. Ji, H. Li, F. Guan, D. Zhang, H. Feng and H. Fan, *J. Inorg. Biochem.*, 2017, **166**, 64–67.
119 Y. Lu, L. Li, M. Li, Z. Lin, L. Wang, Y. Zhang, Q. Yin, H. Xia and G. Han, *Bioconjugate Chem.*, 2018, **29**, 2982–2993.
120 P. Li, S. Liu, G. Zhang, X. Yang, W. Cao, X. Gong and X. Xing, *ACS Appl. Bio Mater.*, 2020, **3**, 1105–1115.
121 J. Liang, W. Li, J. Chen, X. Huang, Y. Liu, X. Zhang, W. Shu, B. Lei and H. Zhang, *J. Mater. Chem. A*, 2022, **10**, 23384–23394.
122 Y. Liu, Y. Zhao, S. Guo, D. Qin, J. Yan, H. Cheng, J. Zhou, J. Ren, L. Sun and H. Peng, *Carbohydr. Polym.*, 2024, **346**, 122656.
123 M. J. Meziani, X. Dong, L. Zhu, L. P. Jones, G. E. LeCroy, F. Yang, S. Wang, P. Wang, Y. Zhao and L. Yang, *ACS Appl. Mater. Interfaces*, 2016, **8**, 10761–10766.
124 A. Pandey, A. Devkota, Z. Yadegari, K. Dumenyo and A. Taheri, *Nanomaterials*, 2021, **11**, 2012.
125 L. N. Wu, Y. J. Yang, L. X. Huang, Y. Zhong, Y. Chen, Y. R. Gao, L. Q. Lin, Y. Lei and A. L. Liu, *Carbon*, 2022, **186**, 452–464.
126 Q. Xin, H. Shah, A. Nawaz, W. Xie, M. Z. Akram, A. Batool, L. Tian, S. U. Jan, R. Boddula and B. Guo, *Adv. Mater.*, 2019, **31**, 1804838.
127 V. TK, A. K. Patel and V. Muthuvijayan, *J. Biomater. Sci., Polym. Ed.*, 2023, **34**, 419–434.
128 S. Shen, H. Qi, T. Yi, T. Jing, J. Li, Y. Gao, Q. Zeng and H. Zhao, *J. Mol. Struct.*, 2025, **1322**, 140620.
129 Y. Fu, F. Wang, H. Sheng, M. Xu, Y. Liang, Y. Bian, S. A. Hashsham, X. Jiang and J. M. Tiedje, *Carbon*, 2020, **163**, 360–369.
130 M. K. Ibrahim, A. Haria, N. V. Mehta and M. S. Degani, *Future Med. Chem.*, 2023, **15**, 2113–2141.
131 S. H. Kim, D. Semenya and D. Castagnolo, *Eur. J. Med. Chem.*, 2021, **216**, 113293.
132 A. R. Gomes, C. L. Varela, A. S. Pires, E. J. Tavares-da-Silva and F. M. Roleira, *Bioorg. Chem.*, 2023, **138**, 106600.
133 A. Dong, Y. J. Wang, Y. Gao, T. Gao and G. Gao, *Chem. Rev.*, 2017, **117**, 4806–4862.
134 R. Liu, X. C. Qing, Z. B. Feng, X. M. Zhang, Y. Zhang, M. Y. Zhang, B. Y. Zhu, Y. Li and L. Xie, *Macromol. Rapid Commun.*, 2023, **36**, 564–573.
135 R. Eldawud, A. Wagner, C. Dong, T. A. Stueckle, Y. Rojanasakul and C. Z. Dinu, *NanoImpact*, 2018, **9**, 72–84.
136 A. S. Bati, L. Yu, M. Batmunkh and J. G. Shapter, *Nanoscale*, 2018, **10**, 22087–22139.
137 C. J. Barnett, C. E. Gowenlock, K. Welsby, A. Orbaek White and A. R. Barron, *Nano Lett.*, 2018, **18**, 695–700.
138 S. Khan, P. Jawlikar, S. Lahoti, O. Bhusnure, S. Chitlange and J. Sangshetti, *Curr. Pharm. Des.*, 2021, **27**, 2454–2467.
139 J. Ackermann, J. T. Metternich, S. Herbertz and S. Kruss, *Angew. Chem., Int. Ed.*, 2022, **61**, e202112372.
140 M. R. M. Radzi, N. A. Johari, W. F. A. W. M. Zawawi, N. A. Zawawi, N. A. Latiff, N. A. N. N. Malek, A. A. Wahab, M. I. Salim and K. Jemon, *Biomater. Adv.*, 2022, **134**, 112586.
141 T. Mocan, C. T. Matea, T. Pop, O. Mosteanu, A. D. Buzoianu, S. Suciu, C. Puia, C. Zdrehus, C. Iancu and L. Mocan, *Cell. Mol. Life Sci.*, 2017, **74**, 3467–3479.
142 S. Kang, M. Pinault, L. D. Pfefferle and M. Elimelech, *Langmuir*, 2007, **23**, 8670–8673.
143 S. Kang, M. Herzberg, D. F. Rodrigues and M. Elimelech, *Langmuir*, 2008, **24**, 6409–6413.

144 L. M. Pasquini, S. M. Hashmi, T. J. Sommer, M. Elimelech and J. B. Zimmerman, *Environ. Sci. Technol.*, 2012, **46**, 6297–6305.
145 M. Assis, J. R. Santos, M. H. Cipriano, R. Y. Reis, L. K. Ribeiro, L. H. Mascaro, E. Longo and J. Andrés, *Surf. Interfaces*, 2024, **53**, 105074.
146 K. Yan, Y. Qin, J. Xue, J. Wang, G. Wang, N. Wang and Y. Chu, *Chem. Eng. J.*, 2024, **484**, 149363.
147 J. Wang, X. Mu and M. Sun, *Nanomaterials*, 2019, **9**, 218.
148 M. Sang, J. Shin, K. Kim and K. J. Yu, *Nanomaterials*, 2019, **9**, 374.
149 D. Kireev, S. K. Ameri, A. Nederveld, J. Kampfe, H. Jang, N. Lu and D. Akinwande, *Nat. Protoc.*, 2021, **16**, 2395–2417.
150 M. Qin, Y. Xu, H. Gao, G. Han, R. Cao, P. Guo, W. Feng and L. Chen, *ACS Appl. Mater. Interfaces*, 2019, **11**, 35255–35263.
151 J. Han, I. Johnson and M. Chen, *Adv. Mater.*, 2022, **34**, 2108750.
152 Z. Li, W. Zhang and F. Xing, *Int. J. Mol. Sci.*, 2019, **20**, 2461.
153 L. Sun, Y. Zhang, Y. Wang, Y. Yang, C. Zhang, X. Weng, S. Zhu and X. Yuan, *Nanoscale*, 2018, **10**, 1759–1765.
154 H. Gu, H. Tang, P. Xiong and Z. Zhou, *Nanomaterials*, 2019, **9**, 130.
155 Y. Esmaeili, E. Bidram, A. Zarrabi, A. Amini and C. Cheng, *Sci. Rep.*, 2020, **10**, 18052.
156 N. Karki, H. Tiwari, C. Tewari, A. Rana, N. Pandey, S. Basak and N. G. Sahoo, *J. Mater. Chem. B*, 2020, **8**, 8116–8148.
157 A. M. Oliveira, M. Machado, G. A. Silva, D. B. Bitoque, J. Tavares Ferreira, L. A. Pinto and Q. Ferreira, *Nanomaterials*, 2022, **12**, 1149.
158 K. Joshi, B. Mazumder, P. Chattopadhyay, N. S. Bora, D. Goyary and S. Karmakar, *Curr. Drug Delivery*, 2019, **16**, 195–214.
159 D. de Melo-Diogo, R. Lima-Sousa, C. G. Alves and I. J. Correia, *Biomater. Sci.*, 2019, **7**, 3534–3551.
160 W. Hu, C. Peng, W. Luo, M. Lv, X. Li, D. Li, Q. Huang and C. Fan, *ACS Nano*, 2010, **4**, 4317–4323.
161 Y. Liu, J. Wen, Y. Gao, T. Li, H. Wang, H. Yan, B. Niu and R. Guo, *Appl. Surf. Sci.*, 2018, **436**, 624–630.
162 R. K. Matharu, T. A. Tabish, T. Trakoolwilaiwan, J. Mansfield, J. Moger, T. Wu, C. Lourenço, B. Chen, L. Ciric and I. P. Parkin, *J. Colloid Interface Sci.*, 2020, **571**, 239–252.
163 X. Guo, X. Zhang, M. Yu, Z. Cheng, Y. Feng and B. Chen, *J. Colloid Interface Sci.*, 2024, **661**, 802–814.
164 A. Chatterjee, E. Perevedentseva, M. Jani, C. Y. Cheng, Y. S. Ye, P. H. Chung and C. L. Cheng, *J. Biomed. Opt.*, 2015, **20**, 051014.
165 H. Wang, M. Zhang, Y. Ma, B. Wang, M. Shao, H. Huang, Y. Liu and Z. Kang, *J. Mater. Chem. B*, 2020, **8**, 2666–2672.
166 J. Wang, Y. Wei, X. Shi and H. Gao, *RSC Adv.*, 2013, **3**, 15776–15782.
167 V. T. Pham, V. K. Truong, M. D. Quinn, S. M. Notley, Y. Guo, V. A. Baulin, M. Al Kobaisi, R. J. Crawford and E. P. Ivanova, *ACS Nano*, 2015, **9**, 8458–8467.
168 J. Shangguan, Z. Wu, C. Qiao, Y. Zhang, L. Li, Q. Li, Y. Gao, H. Yan and W. Liu, *ACS Omega*, 2024, **9**, 7034–7042.
169 Z. Ruan, Z. Xu, T. Liu, L. Chen, X. Liu, K. Chen and C. Zhao, *Heliyon*, 2024, **10**, e38177.
170 D. Zhao, H. Liu, M. Xu, C. Yin, X. Xiao and K. Dai, *Spectrochim. Acta, Part A*, 2024, **314**, 124195.
171 J. Wang, Y. Wang, H. Zhang, W. Zhu and L. Liu, *Exp. Biol. Med.*, 2023, **248**, 2227–2236.
172 H. Li, J. Huang, Y. Song, M. Zhang, H. Wang, F. Lu, H. Huang, Y. Liu, X. Dai, Z. Gu, Z. Yang, R. Zhou and Z. Kang, *ACS Appl. Mater. Interfaces*, 2018, **10**, 26936–26946.
173 M. Mortimer, Y. Wang and P. A. Holden, *Front. Bioeng. Biotechnol.*, 2021, **9**, 683520.
174 G. E. Villalpando-Rodriguez and S. B. Gibson, *Oxid. Med. Cell. Longevity*, 2021, **2021**, 9912436.
175 S. Gurunathan, J. W. Han, A. A. Dayem, V. Eppakayala and J. H. Kim, *Int. J. Nanomed.*, 2012, **7**, 5901–5914.
176 C. D. Vecitis, K. R. Zodrow, S. Kang and M. Elimelech, *ACS Nano*, 2010, **4**, 5471–5479.
177 W. Bing, H. Sun, Z. Yan, J. Ren and X. Qu, *Small*, 2016, **12**, 4713–4718.
178 T. Cui, Y. Fan, Y. Liu, X. Fan, Y. Sun, G. Cheng and J. Cheng, *Foods*, 2023, **13**, 67.
179 R. Rosato, G. Santarelli, A. Augello, G. Perini, M. De Spirito, M. Sanguinetti, M. Papi and F. De Maio, *Int. J. Mol. Sci.*, 2024, **25**, 8033.
180 L. Sun, Y. Zhao, H. Peng, J. Zhou, Q. Zhang, J. Yan, Y. Liu, S. Guo, X. Wu and B. Li, *J. Nanobiotechnol.*, 2024, **22**, 210.
181 W. Xia, Z. Wu, B. Hou, Z. Cheng, D. Bi, L. Chen, W. Chen, H. Yuan, L. Koole and L. Qi, *Mater. Today Bio*, 2025, **30**, 101428.
182 J. W. Kim, E. V. Shashkov, E. I. Galanzha, N. Kotagiri and V. P. Zharov, *Lasers Surg. Med.*, 2007, **39**, 622–634.
183 S. Tan, X. Wu, Y. Xing, S. Lilak, M. Wu and J. X. Zhao, *Colloids Surf., B*, 2020, **185**, 110616.
184 R. Sun, H. Chen, L. Sutrisno, N. Kawazoe and G. Chen, *Sci. Technol. Adv. Mater.*, 2021, **22**, 404–428.
185 B. Z. Ristic, M. M. Milenkovic, I. R. Dakic, B. M. Todorovic-Markovic, M. S. Milosavljevic, M. D. Budimir, V. G. Paunovic, M. D. Dramicanin, Z. M. Markovic and V. S. Trajkovic, *Biomaterials*, 2014, **35**, 4428–4435.
186 W. S. Kuo, H. H. Chen, S. Y. Chen, C. Y. Chang, P. C. Chen, Y. I. Hou, Y. T. Shao, H. F. Kao, C. L. L. Hsu and Y. C. Chen, *Biomaterials*, 2017, **120**, 185–194.
187 W. S. Kuo, Y. T. Shao, K. S. Huang, T. M. Chou and C. H. Yang, *ACS Appl. Mater. Interfaces*, 2018, **10**, 14438–14446.
188 M. Zühlke, T. T. Meiling, P. Roder, D. Riebe, T. Beitz, I. Bald, H.-G. Löhmannsröben, T. Janßen, M. Erhard and A. Repp, *ACS Omega*, 2021, **6**, 23742–23749.
189 P. Kadyan, P. Thillai Arasu and S. K. Kataria, *Int. J. Biomater.*, 2024, **2024**, 2626006.
190 M. P. Mingeot-Leclercq and J. L. Décout, *MedChemComm*, 2016, **7**, 586–611.
191 Y. Tu, M. Lv, P. Xiu, T. Huynh, M. Zhang, M. Castelli, Z. Liu, Q. Huang, C. Fan and H. Fang, *Nat. Nanotechnol.*, 2013, **8**, 594–601.
192 X. Liu and K. L. Chen, *Langmuir*, 2015, **31**, 12076–12086.

193 P. Yi and K. L. Chen, *Environ. Sci. Technol.*, 2013, **47**, 5711–5719.
194 W. Zhu, A. von dem Bussche, X. Yi, Y. Qiu, Z. Wang, P. Weston, R. H. Hurt, A. B. Kane and H. Gao, *Proc. Natl. Acad. Sci. U. S. A.*, 2016, **113**, 12374–12379.
195 T. Mashino, N. Usui, K. Okuda, T. Hirota and M. Mochizuki, *Bioorg. Med. Chem.*, 2003, **11**, 1433–1438.
196 M. Wu, R. Kempaiah, P. J. J. Huang, V. Maheshwari and J. Liu, *Langmuir*, 2011, **27**, 2731–2738.
197 J. Liu, S. Fu, B. Yuan, Y. Li and Z. Deng, *J. Am. Chem. Soc.*, 2010, **132**, 7279–7281.
198 Y. J. Li, S. G. Harroun, Y. C. Su, C. F. Huang, B. Unnikrishnan, H. J. Lin, C. H. Lin and C. C. Huang, *Adv. Healthcare Mater.*, 2016, **5**, 2545–2554.
199 Y. Yao, T. Zhang and M. Tang, *Environ. Pollut.*, 2023, **317**, 120676.
200 I. E. M. Carpio, C. M. Santos, X. Wei and D. F. Rodrigues, *Nanoscale*, 2012, **4**, 4746–4756.
201 J. Chen, H. Peng, X. Wang, F. Shao, Z. Yuan and H. Han, *Nanoscale*, 2014, **6**, 1879–1889.
202 M. Dallavalle, M. Calvaresi, A. Bottoni, M. Melle-Franco and F. Zerbetto, *ACS Appl. Mater. Interfaces*, 2015, **7**, 4406–4414.
203 H. Chen, B. Wang, D. Gao, M. Guan, L. Zheng, H. Ouyang, Z. Chai, Y. Zhao and W. Feng, *Small*, 2013, **9**, 2735–2746.
204 J. Qi, T. Zhang, R. Zhang, J. Liu, M. Zong, Q. Zhang, Y. Ping, Y. Gong, B. Zhang and X. Liu, *Sustainable Mater. Technol.*, 2024, **41**, e01087.
205 Y. Wang, T. Li, L. Lin, D. Wang and L. Feng, *RSC Adv.*, 2024, **14**, 27873–27882.
206 S. Zhang, L. Wang, T. Xu and X. Zhang, *ACS Appl. Mater. Interfaces*, 2023, **15**, 9110–9119.
207 J. Liu, S. Lu, Q. Tang, K. Zhang, W. Yu, H. Sun and B. Yang, *Nanoscale*, 2017, **9**, 7135–7142.
208 G. Liang, H. Shi, Y. Qi, J. Li, A. Jing, Q. Liu, W. Feng, G. Li and S. Gao, *Int. J. Nanomed.*, 2020, **15**, 5473–5489.
209 T. J. Simmons, S. H. Lee, T. J. Park, D. P. Hashim, P. M. Ajayan and R. J. Linhardt, *Carbon*, 2009, **47**, 1561–1564.
210 H. Z. Zardini, A. Amiri, M. Shanbedi, M. Maghrebi and M. Baniadam, *Colloids Surf., B*, 2012, **92**, 196–202.
211 X. Dong, E. McCoy, M. Zhang and L. Yang, *J. Environ. Sci.*, 2014, **26**, 2526–2534.
212 S. Aslan, M. Deneufchatel, S. Hashmi, N. Li, L. D. Pfefferle, M. Elimelech, E. Pauthe and P. R. Van Tassel, *J. Colloid Interface Sci.*, 2012, **388**, 268–273.
213 M. Wang, Y. Su, Y. Liu, Y. Liang, S. Wu, N. Zhou and J. Shen, *J. Colloid Interface Sci.*, 2022, **608**, 973–983.
214 X. Bai, X. Zhang, J. Xiao, X. Lin, R. Lin, R. Zhang, X. Deng, M. Zhang, W. Wei, B. Lan, S. Weng and M. Chen, *Adv. Healthcare Mater.*, 2024, **13**, 2302873.
215 M. Mazaheri, O. Akhavan and A. Simchi, *Appl. Surf. Sci.*, 2014, **301**, 456–462.
216 S. Faghihi, M. Gheysour, A. Karimi and R. Salarian, *J. Appl. Phys.*, 2014, **115**, 244307.
217 W. Z. Weng, Study on the treatment of infectious bone defects and wound scars after open fractures with carbon nanomaterials, PhD thesis, Second Military Medical University of the Chinese People's Liberation Army, Shanghai, 2017.
218 Y. Ma, D. Bai, X. Hu, N. Ren, W. Gao, S. Chen, H. Chen, Y. Lu, J. Li and Y. Bai, *ACS Appl. Mater. Interfaces*, 2018, **10**, 3002–3010.
219 N. K. de Moura, G. F. d. M. Morgado, E. F. Martins, C. A. Escanio, E. Esposito, J. Marini and F. R. Passador, *Macromol. Symp.*, 2022, **406**, 2200020.
220 R. Gayathri, K. ArulJothi, K. H. Raj and S. Gnanavel, *Results Surf. Interfaces*, 2024, **17**, 100287.
221 X. Zhang, X. Bai, X. Deng, K. Peng, Z. Zheng, J. Xiao, R. Zhang, Z. Huang, J. Huang, M. Chen and S. Weng, *Carbon*, 2023, **213**, 118229.
222 Á. Serrano-Aroca, K. Takayama, A. Tuñón-Molina, M. Seyran, S. S. Hassan, P. Pal Choudhury, V. N. Uversky, K. Lundstrom, P. Adadi and G. Palù, *ACS Nano*, 2021, **15**, 8069–8086.
223 Y. Wu, C. Li, H. C. van der Mei, H. J. Busscher and Y. Ren, *Antibiotics*, 2021, **10**, 623.
224 C. Zhang, L. Zhang, X. Liu, L. Chen, Y. Yang and S. Yu, *Mater. Rev.*, 2020, **34**, 53–57.
225 R. Teixeira-Santos, L. C. Gomes, R. Vieira, F. Sousa-Cardoso, O. S. Soares and F. J. Mergulhão, *Nanomaterials*, 2023, **13**, 2604.
226 Y. Li, X. Liu and T. Wu, *China Environ. Sci.*, 2021, **41**, 4402–4414.
227 I. S. Raja, S.-J. Song, M. S. Kang, Y. B. Lee, B. Kim, S. W. Hong, S. J. Jeong, J.-C. Lee and D.-W. Han, *Nanomaterials*, 2019, **9**, 1214.
228 M. Kim, D. Goerzen, P. V. Jena, E. Zeng, M. Pasquali, R. A. Meidl and D. A. Heller, *Nat. Rev. Mater.*, 2024, **9**, 63–81.
229 Z. Peng, X. Liu, W. Zhang, Z. Zeng, Z. Liu, C. Zhang, Y. Liu, B. Shao, Q. Liang, W. Tang and X. Yuan, *Environ. Int.*, 2020, **134**, 105298.
230 S. Chen, Y. Jiang, Z. Zhu, Q. Zhang, C. Zhang, Q. Zhang, W. Qian, S. Zhang and F. Wei, *Adv. Sci.*, 2024, **11**, 2306355.
231 N. Nasirzadeh, Y. Mohammadian, Y. Rasoulzadeh, M. Rezazadeh Azari and F. Khodagholi, *Tanaffos*, 2022, **21**, 391–400.
232 Y. Chiou, C. Lin, S. Harroun, Y. Chen, L. Chang, A. Wu, F. Chang, Y. Lin, H. Lin, A. Anand, B. Unnikrishnan, A. Naing and C. Huang, *Nanoscale*, 2022, **14**, 11719–11730.
233 M. Zhang, Y. Wang, C. Miao, S. Lin, Y. Zheng, X. Lin, Y. Wang, X. Lin, X. Zhu and S. Weng, *Acta Biomater.*, 2025, **200**, 591–609.